

Hydrodynamics of Waves Attenuation Techniques



By

Ikrma Shafiq

(MS WRE&M 2020, 00000330429)

Department of Water Resources Engineering and Management

NUST Institute of Civil Engineering

School of Civil and Environmental Engineering

National University of Sciences and Technology (NUST)

Sector H-12, Islamabad, Pakistan

(2024)

Hydrodynamics of Waves Attenuation Techniques



By

Ikrma Shafiq

(MS WRE&M 2020, 00000330429)

A thesis submitted to the National University of Sciences and Technology, Islamabad, in partial

fulfillment of the requirements for the degree of

Master of Science in Water Resources Engineering and Management.

Thesis Supervisor: Dr. Hamza Farooq Gabriel

Co Supervisor: Dr. Muhammad Israr Siddiqui

NUST Institute of Civil Engineering

School of Civil and Environmental Engineering

National University of Sciences & Technology (NUST)

Islamabad, Pakistan

THESIS ACCEPTANCE CERTIFICATE

Certified that final copy of MS Thesis written by Mr. Ikrma Shafiq., Registration No. MS WRE&M 2020, 00000330429, of batch of 2020, NUST Institute of Civil Engineering has been vetted by undersigned, found complete in all respects as per NUST Statutes/ Regulations/ MS Policy, is free of plagiarism, errors, and mistakes and is accepted as partial fulfillment for award of MS degree in Water Resources Engineering and Management.

Signature: H. F. Gabriel

Supervisor: Dr. Hamza Farooq Gabriel

Date: 16/09/2024

Signature (HOD): [Signature]
HoD Water Resources Engineering and Management
MUST Institute of Civil Engineering
Date: [Signature]
School of Civil & Environmental Engineering
National University of Sciences and Technology

Signature (Associate Dean): [Signature]
Dr. S. Muhammad Jamil
Associate Dean
NICE, SCEE, NUST
Date: 16/9/2024

Signature (Principal & Dean): [Signature]
PROF DR MUHAMMAD IRFAN
Principal & Dean
SCEE, NUST
Date: 16 SEP 2024

National University of Sciences and Technology

MASTER'S THESIS WORK

We hereby recommend that the dissertation prepared under our Supervision by:
Ikrma Shafiq (00000330429).
 Titled: **Hydrodynamics of Waves Attenuation Techniques** be accepted in partial fulfillment of the requirements for the award of Master of Science degree with (B¹ Grade).

Examination Committee Members

1. Name: Dr. Muhammad Israr Siddiqui

Signature: 

2. Name: Dr. Sajjad Haider

Signature: 

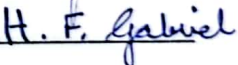
2. Name: Dr. Ammara Mubeen

Signature: 


2. Name: Dr. Majid Ali

Signature: 

Supervisor's name: Dr. Hamza Farooq Gabriel

Signature: 

Date: 16/09/2024


 Head of Department Management
 MUST Institute of Civil Engineering
 School of Civil & Environmental Engineering
 National University of Sciences and Technology
 Dated: 16/09/24


 Associate Dean
 NICE, SCEE, NUST

COUNTERSIGNED

Date: 16 SEP 2024


 Principal & Dean
 PROF DR MUHAMMAD IRFAN
 Principal & Dean
 SCEE, NUST

Certificate of Approval

This is to certify that the research work presented in this thesis, entitled "Hydrodynamics of Waves Attenuation Techniques" was conducted by Mr. Ikrama Shafiq under the supervision of Dr. Hamza Farooq Gabriel.

No part of this thesis has been submitted anywhere else for any other degree. This thesis is submitted to the (Department of Water Resources Engineering and Management, National University of Science and Technology) in partial fulfillment of the requirements for the degree of Master of Science in Field of Water Resources Engineering and Management.

Student Name: Ikrama Shafiq

Signature: 


Examination Committee:

a) GEC Member 1: Dr. Ammara Mubeen

Signature: 

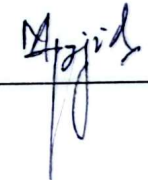
Assistant Professor (NICE, NUST)

b) GEC Member 2: Dr. Sajjad Haider

Signature: 

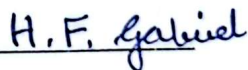
Assistant Professor (NICE, NUST)

c) GEC Member 3: Dr. Majid Ali

Signature: 

Associate Professor (USPCASE, NUST)


Supervisor Name: Dr. Hamza Farooq Gabriel

Signature: 

Co Supervisor Name: Dr. Muhammad Israr Siddiqui

Signature: 


Name of HOD: Dr. Sajjad Haider

Signature: 
HoD Water Resources Engineering and Management
NUST Institute of Civil Engineering
School of Civil & Environmental Engineering
National University of Sciences and Technology

Name of Associate Dean: Dr. S. Muhammad Jamil

Signature: 
Dr. S. Muhammad Jamil
Associate Dean
NICE, SCEE, NUST


Name of Principal & Dean: Prof. Dr. Muhammad Irfan

Signature: 
PROF DR MUHAMMAD IRFAN
Principal & Dean
SCEE, NUST

Author's Declaration

I Ikma Shafiq hereby state that my MS thesis titled “Hydrodynamics of Waves Attenuation Techniques” is my own work and has not been submitted previously by me for taking any degree from this University NUST or anywhere else in the country/ world.

At any time if my statement is found to be incorrect even after I graduate, the university has the right to withdraw my MS degree.

Name of Student: Ikma Shafiq 

Date: 08-06-2024

Plagiarism Undertaking

I solemnly declare that research work presented in the thesis titled “Hydrodynamics of Waves Attenuation Techniques” is solely my research work with no significant contribution from any other person. Small contribution/ help wherever taken has been duly acknowledged and that complete thesis has been written by me.

I understand the zero-tolerance policy of the HEC and National University of Science and Technology towards plagiarism. Therefore, I as an author of the above titled thesis declare that no portion of my thesis has been plagiarized and any material used as reference is properly referred/cited.

I undertake that if I am found guilty of any formal plagiarism in the above titled thesis even after award of MS degree, the University reserves the rights to withdraw/revoke my MS degree and that HEC and the University has the right to publish my name on the HEC/University website on which names of students are placed who submitted plagiarized thesis.

Student/Author Signature 

Name: Ikrma Shafiq

DEDICATION

Dedicated to my beloved Parents, Family and Teachers for their unwavering support throughout my academic journey.

ACKNOWLEDGEMENTS

All praises to **Allah**, the most Gracious and the most Merciful, who bestowed upon me love, knowledge, passion, and strength to complete this research.

Nobody has been more important to me in the pursuit of this degree than the members of my family. I would like to thank my parents, whose love and guidance are with me in whatever I pursue. Without my Father **Dr. Shafiq Ahmad** continuous encouragement and constant support, -I could not have finished this thesis who always provided me financial and spiritual assistance.

I am especially indebted to my supervisor **Dr. Hamza Farooq Gabriel** for his unwavering assistance, incredible enthusiasm, valuable feedback, and astute motivation. Words cannot express my gratitude and profound admiration for him.

I would like to extend my heartfelt gratitude to my co-supervisor, **Dr. Muhammad Israr Siddiqui** for his enlightening guidance during my research work. He provided extensive and professional guidance that I needed to decide on the best course of action for completing my dissertation.

Additionally, I would like to thank to my GEC members **Dr. Majid Ali, Dr. Sajjad Haider** and **Dr. Ammara Mubeen** for their immense help, technical know-how, and moral support.

ABSTRACT

The primary focus of the subject thesis is the pressing necessity to safeguard coastal communities against the increasing risks that marine floods and tsunamis pose. The study looks closely at wave dissipation techniques in an effort to identify workable ways to mitigate these natural disasters. The two main forms of breakwaters are semicircular breakwaters (SCBW) and triangle breakwaters (TBW), whose dissipation tendencies and associated situations are carefully investigated & analyzed. To compare wave dissipation tendencies of these two breakwaters under various situations is the outset of the study. The outcomes constantly demonstrate how well SCBW performed in reducing the effects of waves in variation of scenarios.

Subsequent research focuses on the impact of breakwater perforations on breakwater affectability, determining ideal porosities, and verifying the superior wave dissipation capacities of semicircular breakwater over Triangular breakwater. These studies emphasize the critical role that breakwater's location, porosity, and design play in enhancing resilience to marine disasters and provide valuable insights into effective coastal protection measures. This study examines the impact of the breakwater's location in relation to the shoreline on its dissipation tendencies. Most effective placement strategies are identified following widespread testing. Furthermore, the Shoreline Elevation Index (SEI), a novel non-dimensional statistic, is introduced. An empirical investigation is conducted into the relationship between Shoreline Elevation Index and percentage dissipation by placing breakwaters at nine distinct different positions from shore. Statistical analysis is utilized to confirm the experimental results by building a linear regression model and examining the relationship between shoreline elevation index, Z/Ls and wave dissipation tendencies using IBM SPSS Statistics 26.

Keywords: Semicircular Breakwaters (SCBW), Triangle Breakwaters (TBW), Shoreline Elevation Index (SEI), Porosities.

TABLE OF CONTENTS

LIST OF TABLES	xiii
LIST OF FIGURES	xv
LIST OF ACRONYMS	xvii
Chapter 1: INTRODUCTION	1
1.1 Background	1
1.2 Statement of Problem.....	2
1.3 Scope of Study	3
1.4 Objectives	3
1.5 Significance of the Study	4
1.6 Organization of Research.....	5
Chapter 2: LITERATURE REVIEW	6
2.1 General	6
2.2 Impacts of High Tides on Sea Shores	6
2.3 Previous Studies.....	8
Chapter 3: RESEARCH METHODOLOGY	22
3.1 Experimental Setup.....	22
3.1.1 Introduction.....	22
3.1.2 Hydraulic Flume	25
3.1.3 Wave Maker.....	26
3.1.4 Image recording	28
3.1.5 Breakwater Models	29
3.1.5.1 Triangular Breakwater (TBW).....	29
3.1.5.2 Semicircular Breakwater (SCBW).....	30

3.2	Measurement Techniques	32
Chapter 4: RESULTS AND DISCUSSIONS		38
4.1	Impermeable Breakwaters	38
4.2	Permeable Breakwaters.....	44
4.2.1	SCBW-2 and TBW-2.....	44
4.2.2	SCB-3 and TBW-3.....	48
4.2.3	SCB-4 and TBW-4.....	52
4.3	Summary of Results.....	55
4.4	Effect of Position of Breakwater on Wave Dissipation Tendencies.....	57
4.4.1	Statistical Analysis.....	65
4.4.1.1	R-square	65
4.4.1.2	ANOVA table	67
4.4.1.3	Coefficient table.....	71
Chapter 5: CONCLUSION AND RECOMMENDATIONS		75
5.1	Conclusions.....	75
5.2	Recommendations.....	76
References		78

LIST OF TABLES

Table 3.1: Wave heights in relation to wave period and depth.....	28
Table 3.2: Breakwater model types w.r.t porosities.....	32
Table 3.3: Experimental model scales.....	33
Table 4.1: Wave dissipation percentages of both breakwater in impermeable form.....	39
Table 4.7: Relation of wave attenuation tendencies with location of breakwater for SCBW-3.....	60
Table 4.8: Relation of wave attenuation tendencies with location of breakwater for SCBW-4....	60
Table 4.9: Relation of wave attenuation tendencies with location of breakwater for impermeable TBW-1.....	61
Table 4.10: Relation of wave attenuation tendencies with location of breakwater for TBW-2...	61
Table 4.11: Relation of wave attenuation tendencies with location of breakwater for TBW-3...	62
Table 4.12: Relation of wave attenuation tendencies with location of breakwater for TBW-4...	62
Table 4.13: R square for SCBW-1.....	66
Table 4.14: R square for SCBW-2.....	66
Table 4.15: R square for SCBW-3.....	66
Table 4.16: R square for SCBW-4.....	66

Table 4.17: R square for TBW-1.....	66
Table 4.18: R square for TBW-2.....	67
Table 4.19: R square for TBW-3.....	67
Table 4.20: R square for TBW-4.....	67
Table 4.21: ANOVA results for SCBW-1.....	68
Table 4.22: ANOVA results for SCBW-2.....	68
Table 4.23: ANOVA results for SCBW-3.....	69
Table 4.24: ANOVA results for SCBW-4.....	69
Table 4.25: ANOVA results for TBW-1.....	69
Table 4.26: ANOVA results for TBW-2.....	70
Table 4.27: ANOVA results for TBW-3.....	70
Table 4.28: ANOVA results for TBW-4.....	70
Table 4.30: Coefficient table for SCBW-2.....	71
Table 4.31: Coefficient table for SCBW-3.....	71
Table 4.32: Coefficient table for SCBW-4.....	72
Table 4.33: Coefficient table for TBW-1.....	72
Table 4.34: Coefficient table for TBW-2.....	72
Table 4.35: Coefficient table for TBW-3.....	73
Table 4.36: Coefficient table for TBW-4.....	73

LIST OF FIGURES

Figure 3.1: Hydraulic Flume.....	22
Figure 3.2: Experimental setup.....	23
Figure 3.3: Hydraulic flume schematic diagram.....	24
Figure 3.4: Top view of hydraulic flume.....	26
Figure 3.5: Side view of hydraulic flume.....	26
Figure 3.6: Wave maker.....	27
Figure 3.7: Frequency regulator.....	27
Figure 3.8: Triangular breakwater.....	29
Figure 3.9: Semicircular breakwater.....	29
Figure 10: Permeable triangular breakwater.....	30
Figure 3.11: Real time triangular breakwater models.....	30
Figure 3.12: Permeable semicircular breakwater.....	31
Figure 3.13: Real time semicircular breakwater models.....	31
Figure 3.14: Adjusting the frequency of Wave generator.....	34
Figure 3.15: Horizontal as well as vertical scale with the help of which difference in wave parameters are quantified.....	31

Figure 3.16: Incoming waves encountering Semicircular Breakwater (SCBW).....	31
Figure 4.1: Coefficient of reflection.....	42
Figure 4.2: Coefficient of transmission.....	42
Figure 4.3: Coefficient of dissipation.....	43
Figure 4.4: Relation of wave energy dissipation and incoming wave energy.....	43
Figure 4.5: Relation btw Relative freeboard & Coefficient of reflection.....	47
Figure 4.6: Relation btw Relative freeboard & Coefficient of Transmission.....	47
Figure 4.7: Relation btw Relative freeboard & coefficient of dissipation.....	48
Figure 4.8: Relation btw Relative freeboard & Coefficient of reflection.....	51
Figure 4.9: Relation btw relative freeboard & coefficient of transmission.....	51
Figure 4.10: Relation btw relative freeboard & coefficient of dissipation.....	52
Figure 4.11: Relation btw relative freeboard & coefficient of reflection.....	54
Figure 4.12: Relation btw relative freeboard & coefficient of transmission.....	54
Figure 4.13: Relation btw relative freeboard & coefficient of dissipation.....	55
Figure 4.14: Relation btw dissipated wave energy & incoming wave energy.....	56

LIST OF ACRONYMS

A	Amplitude
BW	Breakwater
H_i	Height of incoming waves wave
H_r	Height of reflected wave
H_s/L	Slope of wave
H_t	Height of transmitted wave
HTB	Hollow Triangular Breakwater
K	Wave Number
K_r	Coefficient of reflection
K_t	Coefficient of transmission
K_d	Coefficient of dissipation
L	Distance of breakwater from shore
L_s	Distance from shore
N_L	Scale of length
PBW	Perforated breakwater
R_c/H	Relative freeboard
RMB	Rubble Mound Breakwaters
SEI	Shoreline elevation index
SC	Scale
SC, SCB, SCBW	Semi-circular Breakwater
T	Time period
TB, TBW	Triangular Breakwater
Z	Height of Breakwater
Z/L_s	Shoreline Elevation Index (SEI)
λ	Wavelength

Chapter 1: INTRODUCTION

1.1 Background

A significant problem along the beaches is flooding brought on by hurricanes and other powerful storms. Because of the usually flat topography, these coastal regions are especially vulnerable to [1] storm surge and wave floods. Sea level rise and the potential for increased storm frequency and intensity due to climate change make this issue even more critical. For decades, many structural techniques and approaches have been employed to safeguard seashores, harbors, and beaches.

Historically, a variety of Techniques and structures have been employed to protect coastal areas, such as breakwaters, jetties, bulkheads, groins, and seawalls. Furthermore, a range of plant species have been employed to safeguard coastal areas. These vegetation management strategies are typically applied in less troublesome areas. Breakwaters have shielded harbors and shorelines from the ocean's destructive power for millennia. The main function of a breakwater is to act as a barrier against the waves, absorbing some of its force and preventing sediment from washing ashore.

Breakwaters are frequently constructed to prevent coastal erosion, lessen ship disturbances caused by waves, and protect port facilities from choppy seas. The primary purpose of rubble mound breakwater or RMB, was to protect harbors and coastlines. Rubble mound breakwaters stop coastal drift and severely degrade or accumulate nearby beaches. Furthermore, they restrict free water movement, degrading the harbor's water quality and making it difficult for fish and bottom-dwelling microbes to pass through [2].

Perforated breakwaters were discovered to be a potential solution for these kinds of significant problems. Breakwaters with perforations, also known as perforated breakwaters (PBW), are a great way to protect coastal communities and ports. They are made up of interconnected concrete or granite blocks with well-placed holes or perforations on them positioned parallel to the shore. line.

The porous nature of perforated breakwaters has historically benefited the marine ecosystem by facilitating water movement and nutrient exchange.

The use of perforated breakwaters has expanded and altered over time to provide shorelines and ports with more effective protection, even though semicircular and triangular breakwaters are also available in a multitude of shapes and sizes. The semicircular breakwater is thought to have been designed in Japan in the early 1990s. Compared to traditional breakwaters, they are more affordable, and effective, and they can be installed over coastal areas with no difficulty [3].

The Hollow Triangular Breakwater is a relatively new innovation in breakwater technology. TBW have a steeper angle, usually near 60 degrees. They are very similar to semicircular breakwaters (SCBW). Triangular breakwaters are designed to protect the shoreline from waves that are approaching from a specific direction. Waves are deflected by the breakwater's acute angle, which decreases their impact on the beach. Harbors that are most often subjected to heighthed waves, this kind of barrier is very useful. The Mekong Delta in Vietnam was the first region where this Hollow Triangular breakwater was first employed in its realistic setting [4].

1.2 Statement of Problem

The National Institute of Oceanography (NIO) predicts that Karachi would likely sink in the next 35 to 45 years. According to a warning from the NIO, if prompt action is not taken, areas of Malir have already sunk and 30–40 million people may be relocated because of climate change. Experts have warned that climate change is a bigger threat to the country than terrorism since sea levels are rising by six millimeters annually [5].

The actual resolve of this study is to investigate the necessity of improved harbor & coastal safety protocols. The primary goal is to empirically investigate the effectiveness of wave energy attenuation techniques using linear wave theory on two different kinds of breakwaters.

1.3 Scope of Study

In the subject of coastal protection, research on damage prevention, the exploitation of marine energy resources, and the impacts of offshore waves on coastal regions has become essential. Historically, harbors and shorelines have been protected from flooding by the employment of wave attenuation measures as well as various techniques ranging from employing different types of plant species near the shore as well as building concrete structures specifically, different types of breakwaters as well as sea walls. This subject study focuses on two types of breakwaters; the Semicircular Breakwater (SCB) and the Hollow Triangular Breakwater (HTB). Through a series of real-world experiments, the hydrodynamics of waves as well as wave attenuation tendencies of both the breakwaters are examined by employing different scenarios of water depth at different changed frequencies, changing perforations of breakwater as well as strategically placing breakwaters at different positions with respect to shoreline. The primary goal is to compare these two types of breakwaters' wave dissipation properties.

1.4 Objectives

- The prime goal of this study is to thoroughly compare the effectivity of the two forms of coastal breakwaters: semicircular breakwater and the triangular breakwater in terms of wave attenuation tendencies in their respective forms—permeable and impermeable.

The explicit objectives of the research study are:

- To determine the association between the seaside and shoreside porosity of breakwaters to ascertain the ideal optimum percentage porosity for reducing wave energy.
- To examine how Relative freeboard effects breakwater performance in wave energy dissipation and overtopping tendencies.

- To determine how breakwaters behave in response to varying positions in relation to the coast and how wave dissipation tendencies are affected by changing location of breakwater, finding best optimum location with respect to shore giving minimum wave reflection heights and maximum wave dissipation percentages.
- To carry out a comparative evaluation, employing Linear Wave theory to analyze the performance of both breakwaters concurrently under the same physical conditions.

1.5 Significance of the Study

Today, the need to increase coastal resilience is greater than ever due to climate change's effects on unpredictable weather conditions, plunging floods, and relentless tsunamis. The hazard of climate-induced instability must be addressed more urgently as rising sea levels and temperatures. This work is a contribution in providing creative answers to the ever-present threat posed by sea level rise. This study aims to reduce coastal vulnerability and protect shorelines and harbors by investigating solid and permeable versions of Triangular Breakwater (TBW) and Semicircular Breakwaters (SCBW). The objective is to keep the beach peaceful throughout the climate catastrophe while guaranteeing the security and welfare of individuals residing near the shore.

1.6 Organization of Research

- Chapter 1:

Introduction: Introduction of thesis topic, background, objectives, and significance of the study.

- Chapter 2:

Literature Review: Literature review of past studies on evaluation of gridded datasets, assessment of bias correction methods and development of gridded datasets.

- Chapter 3:

Research Methodology: Experimental setup, apparatus, tools Measurement techniques are discussed.

- Chapter 4:

Results and Discussion: Results and findings are presented and discussed in this chapter.

- Chapter 5:

Conclusion & Recommendations: An overview of the study's findings and recommendations for future research.

Chapter 2: LITERATURE REVIEW

2.1 General

Sea flooding, often known as coastal or sea flooding, is the result of ocean water flooding coastal areas. This might be caused by storms, heavy rainfall, high tides, storm surges, and the consequences of climate change, such as increasing sea levels. Storm surges are one of the main reasons for flooding at sea [6]. Storm surges are the outcome of a storm's powerful winds forcing water toward the coast. Sea levels may temporarily rise if this is combined with low air pressure. There is a significantly greater chance of flooding if these surges occur during high tide. Coastal regions are especially susceptible to the combined effects of high tides and storm surges.

Coastal areas are under risk from rising sea levels brought on by climate change [7]. Ocean levels increase as a result of the melting of glaciers and polar ice caps brought on by warming temperatures due to climate change. The coastal zone is an essential component of human populations and acts as a dynamic link between the terrestrial and marine ecosystems. It also provides habitat to numerous types of vegetation and wildlife.

Sea level rise pose a devastating impact on a region's important infrastructure, including roads and utilities. Coastal flooding frequently results in erosion and flooding, loss of valuable land and erosion of the shoreline. This delicate ecosystem's balance is becoming more and more vulnerable due to the phenomenon of soil erosion along seashores, which become worse by sea level flooding.

2.2 Impacts of High Tides on Sea Shores

High tides are caused by periodic variations in the height of the ocean waves caused by the gravitational attraction of the moon and sun [8]. High tides have a significant effect on the social and environmental aspects of coastal towns. The people who live nearby suffer the most from these lethal storm surges. since they directly jeopardize the stability of seashores. Their occurrence,

which is basically characterized by an increase in sea level and furious sea waves, dramatically exacerbate coastal erosion, changing the surrounding ecology and resulting in the destruction of substantial coastal land.

The local population, particularly those who reside near to the coast are fully or partially impacted by the high tides in the sea. Coastal cities are affected in a number of ways by these tidal variations. High tides increase the likelihood of coastal flooding, particularly when storm surges or unfavorable weather pattern persists. There is danger to homes, livelihoods, and infrastructure, which affects the general well-being of the community. High tides can worsen coastal erosion by slowly eroding shorelines and endangering coastal ecosystems. During high tides, freshwater supplies can be impacted by saltwater intrusion, endangering the community's access to clean drinking water. High tides can occasionally interfere with transportation and communication networks, making daily living and business operations more difficult.

The development and use of coastal zones have a major impact on economic growth of all countries. These places draw curiosity and interest as centers for a variety of human activity. As a result, these places have gone through important developments including the building of commercial, industrial, and residential buildings as well as the development of harbor projects and public infrastructure. Overall, these programs are essential for establishing links between a nation's internal and exterior sectors, but the tidal surges that modify the shoreline may detract from their aesthetic value.

This could discourage tourists and hurt the local economy, which depends heavily on tourism. There are number of countries whose economy directly or indirectly depends upon Tourism. So, making sea calm is very critical in attracting tourist. Furthermore, during high tide, the infrastructure that supports recreational activities—beaches and coastal resorts, for example—is

more susceptible to erosion and destruction. Because of this, the economic repercussions go beyond the local coastal community, having an impact on businesses that rely on tourism and necessitating the development of adaptable solutions to protect coastal economies [9].

The most important parts of the maritime infrastructure, the harbors, are badly affected by high tides. Increased tidal activity may lead to situations that complicate harbor operations and jeopardize maritime safety. The rising water levels brought on by high tides make navigation more difficult, dangerous for ships, and impede effective marine operations. Because harbors are vulnerable to the damaging impacts of high tides, the integrity of these major maritime hubs needs to be protected with strong coastal management strategies.

2.3 Previous Studies

Decades of investigation and analysis have been devoted to lowering high tides and preserving tranquility near the shore. Calming the water has been the main goal of many creative approaches. Various plant species, such as mangroves, coral reefs, saltmarsh grasses, and various trees, have been used as a buffer against high tides on occasion.

Mangroves pose significant help in lowering the risk of wind, furious waves, storm surges, and tsunamis that come with living close to the shore. Mangroves are one of the important types of intertidal wetland that inhabit the area where land and water meet along tropical and subtropical coasts [10]. And at some places these mangrove forests are deliberately grown near the shore in order slow down sea waves.

A researcher examined the effect of mangroves on human fatalities during a 1999 super storm that devastated Orissa, India, using data from several hundred communities. According to the study, communities with more mangrove cover between them and the beach had a significantly lower

fatality rate than areas with little to no mangrove cover. This is because mangroves assist human civilization in considerably more ways than just providing storm protection [11].

Mangroves are generally believed to provide just a small solution to these issues. Little fluctuations in water levels, however, can result in smaller flood zones, which reduces the number of fatalities and property damage. A study introduced the kelp-box floating breakwater, a marine plant that is the focus of her research and necessary for enhancing the maritime environment [12]. A computer model was created to investigate the interaction between waves and the floating barrier. The findings demonstrate that the presence of kelp enhances the floating breakwater's capacity to disperse waves.

Additionally, coral reefs also serve as a defense against heightened waves. Data from field research was used to investigate how coral reefs attenuate ocean waves. It was found that there is observable wave attenuation, and that the attenuation rate agrees with known hypotheses concerning wave breaking decay and bottom friction. Furthermore, once the wave spectrum crosses reefs, it noticeably widens [13]. The protective function of coral reefs reduces the risk of coastal flooding for more than 200 million people [14]. They provide natural barriers against storm surges and high tides, mitigate the effects of the tides and create a more tranquil seaside environment, by taking advantage of the flora's natural resistance [15].

In addition to vegetation, many structural structures are used to stop floods. Coastal defensive structures come in a variety of forms, including jetties, groins, seawalls, breakwaters, and artificial headlands. There are various kinds of breakwaters available: major breakwaters, enormous vertical face breakwaters (block, caisson, cellular forms, rubble mound breakwaters), composite breakwaters (comprising a vertical superstructure of caissons or plain concrete blocks on a sizable rubble mound foundation), and flexible breakwaters (composed of rows of sheet piles or contact

piles). Their goal is to prevent tidal surges and retain water in designated places, hence reducing the likelihood of floods [16].

Breakwaters protect harbor infrastructure from turbulent waves and lessen coastal erosion, among other functions. The first kind of breakwater, known as rubble mounds, has been used extensively to safeguard harbors. The earliest rubble mound barrier was built in the seventh century BC, most likely on the island of Delos. On the other side, Herodotus claims that the more well-known breakwater is older than 530 BC and is situated on Samos [17].

Breakwaters made of rubble mounds are divided into various categories. These include reef-type, near-bed, low-crested (both emergent and submerged), reshaping (berm) breakwaters, and structures that are neither very little overtopped nor overtopped. In the past, RMB breakwaters were the most widely used type of breakwater [18]. In order to examine the physical processes involved in the operation of a prototype rubble mound breakwater against stochastic waves, an equipment was installed on a portion of the Rubble Mound breakwater located at the harbor at Zeebrugge, Belgium. Field data on wave impact in front of the breakwater was evaluated, the hydraulic behavior of the full-scale breakwater, and the pore pressure reaction inside the breakwater core [19].

Numerous researchers have done extensive study on rubble mound breakwaters' efficacy. Creating marine infrastructure is a pricey enterprise compared to other endeavors, according to a scientist that he claimed during his detailed study on RMB. Therefore, cost and manufacturing efficiency become critical in breakwater management [20].

Rubble Mound Breakwater has the potential to obstruct littoral drift, which can severely erode or accrete nearby beaches. In addition, these structures impede the flow of water, which leads to inadequate circulation and reduced water quality in the port, endangering the ecology. They also

provide barriers for fish and other bottom-dwelling microorganisms. Additionally, constructing a rubble mound breakwater can be expensive, particularly in places where the required materials are scarce [21].

To address these kinds of issues perforated breakwaters was first proposed as a remedy for the aforementioned issues. This innovative design has a front wall with perforations, a chamber for dispersing wave energy, and a solid rear wall. In particular, the design of the breakwater facilitates the flow of water and the removal of trash, which keeps the harbor clean and permits fish and microorganisms to pass through. Perforated breakwaters save construction time, enhance hydraulic efficiency, reduce total costs, preserve quality control, account for environmental factors, and simplify maintenance procedures [22].

Since the introduction of perforated breakwaters, numerous changes have been anticipated and tested in order to gain a better understanding of their hydraulic and hydrodynamic features. The purpose of these modifications is to use the wave dissipation technology inside a vertically perforated structure. The functional efficacy of these perforated breakwaters has been studied theoretically, computationally, and empirically by assessing the reflection and transmission coefficients.

A distinctive breakwater was proposed for the coast of Sussex [23]. This breakwater was made up of three parts: a cellular structure with a perforated forward-facing wall, a solid rear wall above the low water line, and a solid base below it. This breakwater's efficacy was evaluated in a flume at Wallingford's Hydraulics Research Station. Wave forces and reflections were noted during the trials, and they were determined to be satisfactory. Similarly, another researcher calculated the transmission and reflection of random waves hitting dissipative breakwater, an analytical model was devised for this specific purpose [24].

In order to calculate the transmission and reflection coefficients of vertical breakwaters with two impervious and permeable perforated slotted walls, analytical model was developed. The experimental data demonstrated a strong degree of agreement, confirming the model's validity. According to the results the least reflection for both kinds of breakwaters can be found at $B/L = 0.25$, where B is the structure's width and L is its wavelength. It was determined that, in comparison to breakwaters of Jarlan's type, impermeable breakwaters with two perforated walls had noticeably lower reflection coefficients [25].

In 1992, a group of researchers conducted a theoretical and experimental investigation of the dispersion of small-amplitude water waves by a series of vertical cylinders with a solid vertical back wall. They included a blockage coefficient to approximate the energy loss caused by flow separation near the cylinders. There was a noticeable level of agreement between the experimental findings and the theoretical conclusions [26].

A theoretical study and numerical simulation were developed to assess the effectiveness of a breakwater consisting of three distinct components: a core filled with rocks, an impermeable back wall, and a perforated front wall. It added a boundary condition at the perforated wall to their numerical model to take energy dissipation into consideration. The model was verified by comparing the outcomes with data from previous numerical investigations. The examination examined wave run-up, wave force, and wave reflection coefficient [27].

In 2000, efficacy of a breakwater featuring a perforated front wall, an impermeable back wall, and a core filled with rock was assessed. In order to take energy dissipation into consideration, an eigenfunction expansion approach was used [28]. Previous research on the extreme situations of permeable seawalls and perforated breakwaters with impermeable rear walls bolstered conclusions

of this study. An example of how to apply the chosen parameters to a real-world design scenario in addition to demonstrating how to model the breakwater's permeability was also presented.

Analytical model to study the dynamics of waves interacting with a slotted seawall was developed. Experimental results validated the model's validity and led to the conclusion that porosity and incident wave height mostly affect the reflection qualities. Based on this research, the diameter of the chamber should be about 25% of the incoming wavelength in order for the reflection coefficient to attain its minimal value [29].

Researcher studied the reflection of waves from oblique incidents. The breakwaters he used had an impermeable rear wall and a two-layer perforated wall. There are three sub-domains within the fluid domain, and each one uses an eigenfunction expansion technique. This work compares numerical findings from the proposed model with experimental data. The study also examines the primary determinants of the reflection coefficient. A numerical comparison was made between the reflection coefficient of a double-layered structure and that of a single-layered one. The results show that the center's perforated wall has a complex effect [30].

In addition to the conventional perforated breakwater, a unique modified perforated breakwater design was presented. This design has a two-layer core filled with rock, with a wave-absorbing chamber situated between a solid back wall and a perforated front wall. Eigenfunction expansion approach was utilized to assess this innovative structure's hydrodynamic performance. Through research, it became possible to solve propagation of waves of water in two-layer porous media. The numerical outcomes of this model were then compared to the limiting scenarios that were previously looked at [31].

Another study examined the behavior of the flow field close to a perforated breakwater and evaluated the breakwater's effectiveness in the presence of regular waves. To assess the efficacy

of the structure, thirteen different types of regular wave scenarios with different wave heights and durations were looked at. The study comprised ten phases each wave to evaluate the flow field fluctuation with phase. A comparison of energy dissipation based on velocity and elevation data is included in the study. The findings showed that energy dissipation was greater than 69% in more than 75% of the wave scenarios that were studied, indicating the structure's notable effectiveness in dispersing energy [32].

The wave flume experiments were carried out at the Universidad Politécnica de Valencia's Laboratory of Port and Coasts. This study looked at the reflection behavior of breakwater caissons with one to three chambers and wall openings.

A total of 1800 regular wave tests and 160 irregular wave tests were performed for both slotted and holed walls. Several simulated laboratory data sets were created and carefully examined in order to evaluate the breakwater reflection performance. It was found that the coefficient of reflection (CR) of the breakwater is highly dependent on its porosity [33].

The hydrodynamic behavior of a vertical wall with horizontal gaps that were permeable at the bottom was examined in further detail. Regular, conventional waves were allowed to interact upon it. Numerous wave and structural properties were looked into. A theoretical model was created using the Least Squares Technique. The findings were contrasted with those from earlier studies in order to verify the theoretical model. The comparison showed that when the friction factor (f) is adjusted to 5.5, the theoretical model predicts wave transmission, reflection, and energy dissipation coefficients accurately. Furthermore, when the relative wavelength (h/L) is greater than 0.3, the model accurately predicts transmission coefficients below 0.5 and reflection coefficients beyond 0.5 [34].

The most recent developments in perforated/slotted breakwater research are presented in a 2011 study. This research focused on two types of these breakwaters: those with impermeable back walls and those without. In addition to measuring wave forces on perforated caissons, scientist has made contributions by looking through a number of recent research that were published in Chinese journals and may not have been discovered by other subject matter specialists. The goal of this endeavor was to support other researchers who are engaged in pertinent researches [35].

Another study analyzed the porous and permeable breakwaters in 2012, concentrating on the physical dynamics of wave–structure interactions. The study focuses on small-holed, highly permeable pipes that promote convection and seawater exchange, hence facilitating wave convection in harbor locations. Through laboratory tests of wave transmission over permeable pipe breakwaters under various wave circumstances and varying combinations of diameter and tube length, the research aimed to understand the dissipation processes of porous vertical pipe breakwaters [36].

A dynamic breakwater concept with a solid rear wall and a perforated front wall was put out. Research was conducted comparing the wave impacts of a perforated breakwater with a caisson-type barrier. Scouring was more common when the caisson-type was attached to the bottom, according to visual observations, although it was not visible when the breakwater is perforated [37]. The primary focus of the investigation is the horizontal wave force delivered to the front and rear walls, together with metrics like the wave transmission coefficient (CT), reflection coefficient (CR), and energy dissipation coefficient (CE). This study looked at the interaction between waves and a number of semi-immersed, hole-filled Jarlan breakwaters. The hydrodynamic parameters of these breakwaters have been evaluated in a computer model and linear wave theory. The coefficient of resistance (CR) of the triple semi-immersed Jarlan-type perforated breakwaters was

substantially lower than that of the double design. This scenario lessens wave forces by improving the structure's ability to absorb waves [38].

Researcher investigated the performance of inclined porous screens in a laboratory flume. Screens with three distinct hole sizes were assessed as part of the study, taking into account the existence of a sluice gate upstream. Various screen inclinations in various flow direction orientations were investigated, all while keeping consistent 40% porosity. Comparing the findings to the screen's tilt, the classic hydraulic leap showed a considerable reduction in energy loss. Nevertheless, there was no discernible effect of changing the screen's tilt on the energy dissipation mechanism. Energy dissipation varies at the same angle, but it has little effect on the flow system [39].

Many types of perforated breakwaters (PBW) have been used to lessen heightened sea waves. In this study, three different kinds of breakwaters were examined under different conditions. The creation of breakwater structures has a long and rich history. Many concepts that blend different building materials and architectures have been tested since the 1960s. Four positional categories are commonly used to categorize breakwater constructions: attached, headland, nearshore, and detached breakwaters [3].

Perforated concrete blocks were proposed as an innovative alternative to traditional breakwaters. The usefulness of these blocks as wave height mitigators was examined in their inquiry. When it comes to breakwaters, perforated concrete blocks make sense when the wave height is decreasing. If these blocks are used to safeguard the coast, the wave height inside the protected area might go down. Additionally, the several holes in the perforated concrete block, lower the amount of concrete and provide habitats for marine life & indicated that this material may find use in both the environmental and economic spheres [40].

Semicircular Breakwaters (SCBW) and Triangular Breakwaters (TBW) are the two types of breakwaters whose dissipation tendencies have been studied in this study. Japan began using semicircular breakwaters in the early 1990s. Between 1992 and 1993, a 36-meter test version of the semicircular breakwater prototype was built in Miyazaki Port. This inventive breakwater design made use of a semicircular vault and a bottom slab made of precast reinforced concrete [41].

The Yangtze River Estuary's Deep Channel Improvement Project completed its first phase in 2000 with the construction of an 18-kilometer semicircular estuary jetty. At China's Tianjin Port, a semicircular wall spanning 527 meters was constructed. Additionally, it was suggested that the semicircular jetty be built during the Deep Channel Improvement Project's second phase for the Yangtze River Estuary [42].

Semicircular breakwaters in their submerged and emergent forms have been the subject of several researches. Yuan examined the wave forces influencing these formations closely. For the semicircular breakwater, this study examined three different hydrodynamic scenarios: submerged, alternatively submerged, and emerging. To validate and refine the numerical model, five sets of laboratory experimental data representing semicircular breakwaters with varying forms and diameters were utilized. The outcomes showed good agreement between the numerical simulations and the experimental data [43].

Submerged breakwaters are frequently utilized in coastal areas, particularly where total wave protection is not required. In addition to safeguarding harbor entrances, these structures also provide artificial fishing grounds and reduce littoral drift. Submerged breakwaters are used in many different configurations in real-world applications; research is conducted on physical models to assess their efficacy [44].

In 2009 research was conducted on scouring phenomenon at the foot vertical and semicircular submerged breakwaters. Trials were carried out in an experimental environment using monochromatic waves that broke at the breakwater on both oblique and plane sandy bottoms. The study's key discovery is that, regardless of the submerged breakwater's particular form or kind, the onshore scour characteristics at the base of the breakwater stay constant [45].

In 2011 researcher studied the effects of vertical and semicircular breakwaters in submerged form on the characteristics of neighboring waves. In the experimental testing, on both horizontal and sloping sandy bottoms, monochromatic waves with normal incidence broke at the breakwater. Providing precise parameterizations for the wave reflection coefficient computation is the main objective of the study. The results indicated that the reflection coefficient (C_r) is most significantly influenced by the dimensionless submergence parameter [46].

An investigation into the hydrodynamic properties of a perforated semicircular free surface breakwater (SCB) under irregular wave conditions was conducted in 2010. The study reports on the measured horizontal wave forces operating on the SCB and examined the wave transformation behavior outside and inside the breakwater's chamber. It states that the hydrodynamic performance of the breakwater may be evaluated by using the transmission, reflection, and energy dissipation coefficients. These coefficients are then expressed in terms of the relative breakwater width (B/L_p) and the relative submergence depth (D/d). It is found that the wave attenuation capabilities of the SCB model increase as these ratios climb.

Perforated free surface semicircular breakwater was found to be a highly effective anti-reflection construction with a significant capacity for energy dissipation during experimental testing. It was found that the breakwater's effectiveness decreased as the immersion depth decreased and the wavelength increased. The solution to this issue was to install wave screens beneath the free

surface semicircular caisson with varying designs and porosities to improve the breakwater's performance in circumstances where the immersion depth is limited [47].

Physical modeling was used to investigate the hydrodynamic properties of these compound breakwaters in irregular wave situations. A comparison of experiment results showed that the double-screened semicircular caisson and 25 percent porosity performed better than those with a single screen. It was also observed that longer waves might be more successfully dampened by enlarging the wave screen [48].

Another research studies the behavior of oblique waves on a submerged perforated semicircular breakwater using the linear wave theory. A perforated semicircular arc splits the fluid domain into its inner and outer parts. Numerical studies showed that the semicircular breakwater has lower reflection and transmission coefficients than typical incident wave conditions when the angle of incidence is 45 to 60 degrees. Both horizontal and vertical waves exert greatest forces on the structure, and a discernible phase difference helps the structure resist sliding regardless of the wave angle. When building perforated semicircular breakwaters, choosing the appropriate porosity is essential [49].

Further study examines the Bragg reflection phenomenon by interacting with waves through a large number of submerged semi-circular breakwaters. Incident waves, whether incidental or indirect, are taken into consideration in this study. To determine the breakwaters' transmission and reflection coefficients at various wave times, experiments were carried out. Outcomes of the analysis show a good arrangement with the experimental data. Furthermore, the bandwidth of Bragg reflection and the peak reflection coefficient of particular submerged semi-circular breakwaters are studied in detail using numerical examples [50].

Behavior of submerged semicircular and quarter-circular breakwaters under irregular wave circumstances via wave loading was studied. It was found that a semicircular breakwater's wave force spectrum was similar to that of a quarter-circle barrier. Furthermore, it was demonstrated that irregular waves had a smaller dimensionless peak wave force than regular waves. Using a RANS-VOF model, the impact of submerged breakwaters' local hydrodynamic disturbances on the pressure distribution surrounding the structure and the overall wave load was investigated.

Numerical models show that wave-induced vortices surrounding the structure significantly increase wave stress on the submerged quarter-circular breakwater but have no effect on the semicircular breakwater [51].

In 1996, the Triangular Breakwater's wave change was investigated for the first time. A numerical model was used to study the wave transition. A comparison was made between the results and the experiment's results [52].

A researcher conducted the first test of a revolutionary construction known as the Hollow Triangle Breakwater (HTB) in 2022 with the goal of reducing the effects of coastal erosion and restoring mangrove habitats along the Vietnamese Mekong Delta (VMD) borders. Physical modeling was used to verify and thoroughly evaluate the hydraulic parameters of the HTB. The results showed that the breakwater porosity and reflection coefficient were inversely related. Field observations and experimental data demonstrated that long waves were able to pass through the HTB whereas shortwave radiation was efficiently dispersed. This approach shows how the HTB could mitigate shoreline erosion in the VMD by encouraging silt accumulation and mangrove restoration [4].

The subject study compares the wave dissipation tendencies of two types of breakwaters Semicircular Breakwater and the Triangular Breakwater in their solid and perforated forms. Breakwaters are tested in both emerged and submerged states. Furthermore, the performance of

these breakwaters is evaluated by varying their positions with respect to the shore. Here it is important to mention that concept of percentage perforations for the two breakwaters is adopted from previous study [4].

Chapter 3: RESEARCH METHODOLOGY

3.1 Experimental Setup

3.1.1 Introduction

Tests were carried out on the flow field and the variation in wave heights brought about by the contact of solitary-like monochromatic waves with two kinds and within each type 4 different configurations of breakwaters in submerged and emerged forms, number of experiments are conducted to conduct these inquiries. The hydraulic flume used for these tests is shown in Figure 3.1.



Figure 3.1: Hydraulic Flume

Wave dissipation has been the topic of numerous theoretical and analytical studies in the past, but there hasn't been much work done to physically test these models, especially when employing prototype models like the ones being investigated in current research.

One of the fundamental indicators of the modeling concept when using model scale is the ability to reproduce a problem or phenomenon from a prototype model on a smaller scale. This ensures that the model accurately represents the event in the prototype. There are certain constraints that the model must satisfy based on the observable features of the phenomenon, such as geometric and kinematic similarity. Geometric similarity is the ability of a model and a prototype to have similar shapes even when their sizes may vary. When there is perfect geometric resemblance, there is similarity in the horizontal and vertical length scales [53]. In this study modeled experimental setup used was modeled on the basis of real-world Scenario. A scale from 1 to 256.41 was employed in this study.

The apparatus used in this experimental setup is given below in Figure 3.2

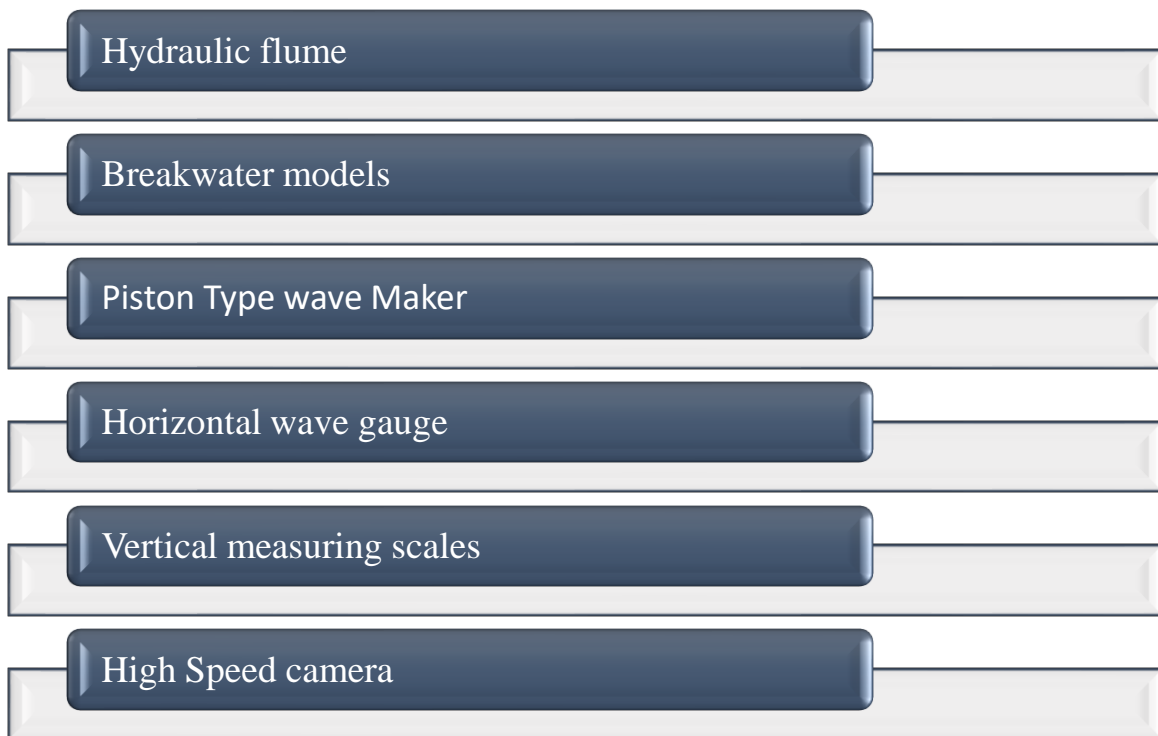


Figure 3.2: Experimental setup

The schematic diagram of the Experimental setup is given below, (Figure 3.3)

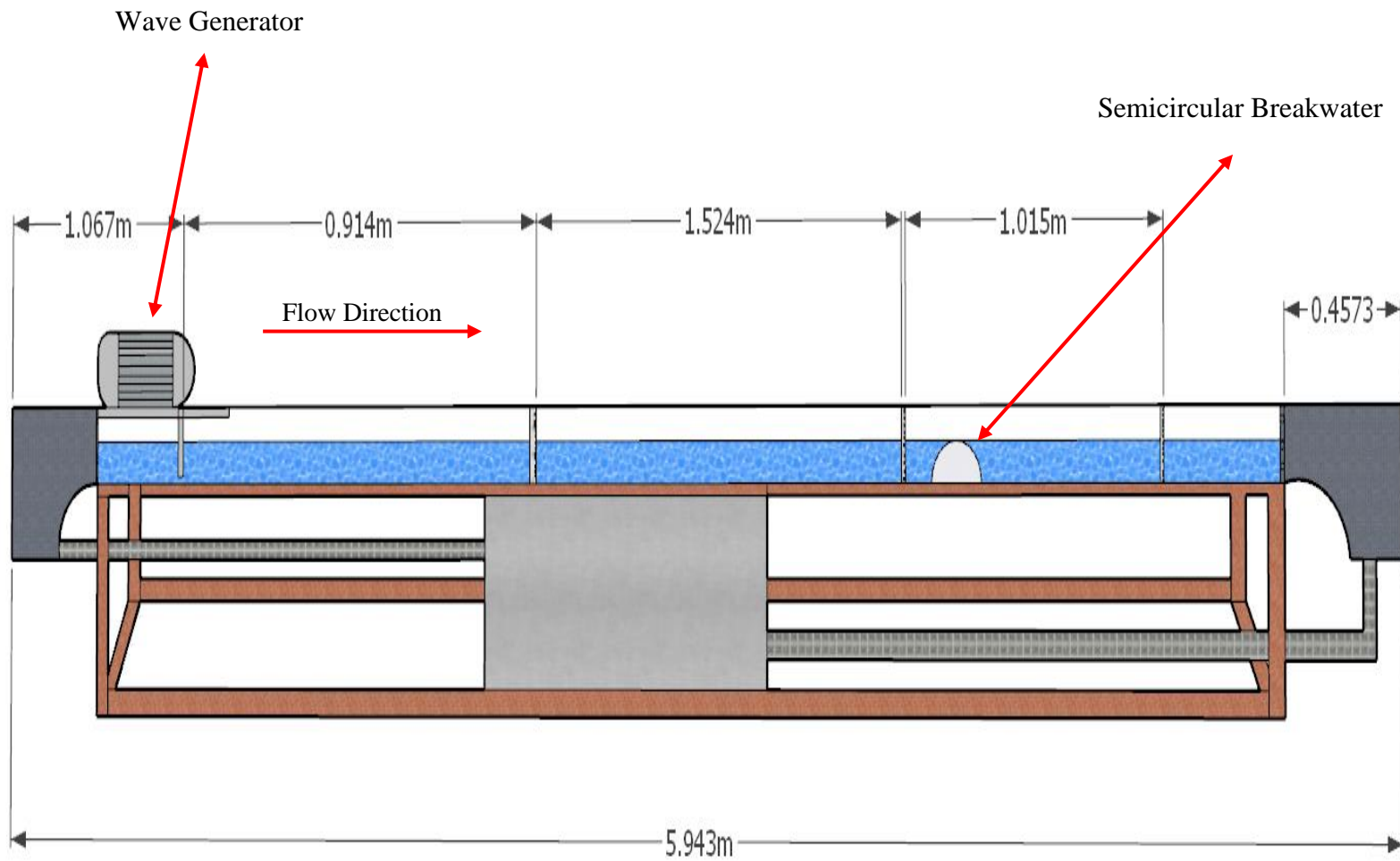


Figure 3.3: Hydraulic flume schematic diagram

3.1.2 Hydraulic Flume

Hydraulic flume is placed in the Hydraulics lab of NUST Institute of Civil Engineering (NICE), School of Civil & Environmental Engineering (SCEE) at the National University of Sciences and Technology (NUST). It has dimensions of 5.94m in length, 0.078m in width, and 0.254m in depth. The walls of this hydraulic flume are made of clear Plexiglas for optical vision, while the structure is made up of steel. To reduce wave reflection and absorb incoming wave energy, the wave flume is provided with horsehair termination layer at the very end of hydraulic flume. Hydraulic flume is divided into portions. Throughout its length, seven measuring scales (numbered SC-1 through SC-7) were arranged at $L/7$ intervals to measure the heights of incoming, reflected, and transmitted waves. Throughout the whole length of the hydraulic flume, a sizable horizontal measuring scale was carefully positioned perpendicular to the vertical axis in order to measure lateral disturbances and other important parameters in the water flow and look into a number of related factors. The water depth was first fixed at 16 cm for all the tests, and it was later changed based on the needs of the experiment. The hydraulic flume was positioned in front of a high-speed camera to record changes in water depth. The schematic diagrams of Hydraulic flume top view and the front view are given below in Figure 3.4 and 3.5.

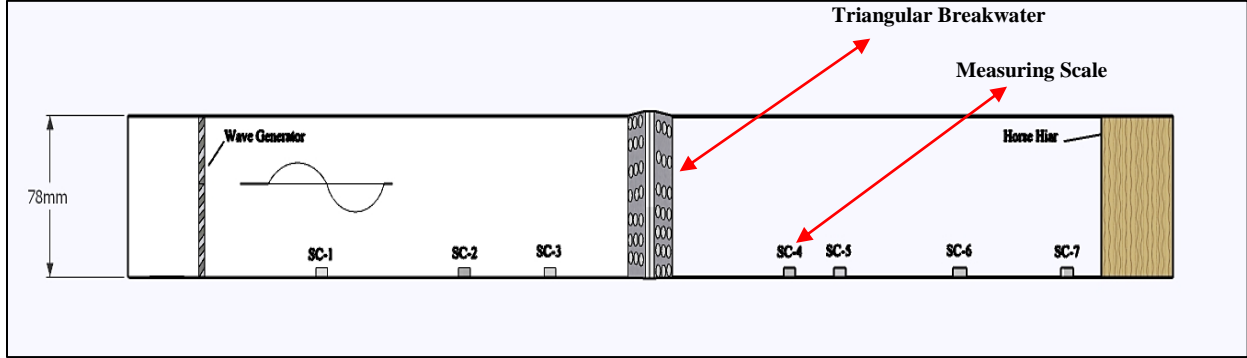


Figure 3.4: Top view of hydraulic flume

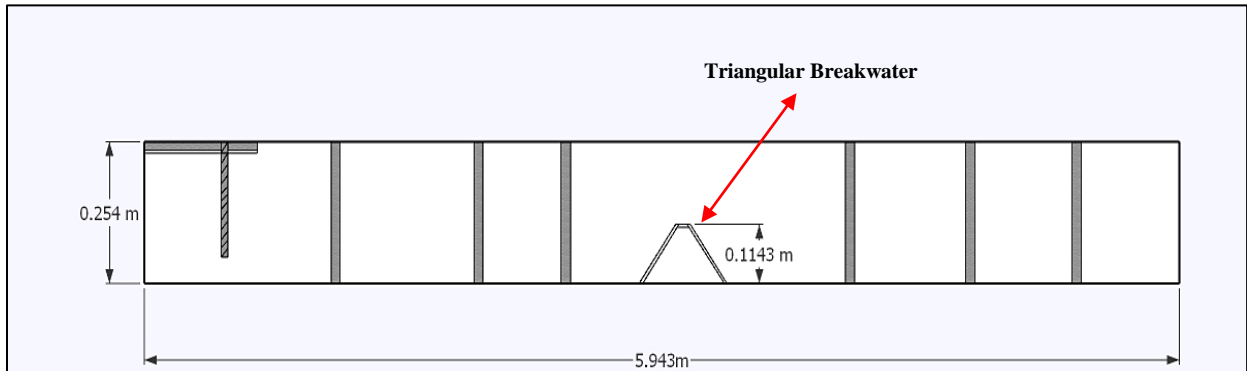


Figure 3.5: Side view of hydraulic flume

3.1.3 Wave Maker

In a natural environment, following little dispersive waves sometimes make it difficult to create a solo wave. In order to study the effects of long waves, a variety of techniques have been used in physical experiments to produce solitary or impulse waves. These techniques include using Scott Russell wave generators, land-sliding systems, and piston-type wave generators, among others [54] [55]. To produce monochromatic waves for the current investigation, a piston-type wave generator was used as can be seen in the Figure 3.6 & 3.7. This wave generator, is placed farthest to the left of the hydraulic flume, has a 0.5 HP power motor and a regulator that enable exact and synchronized correction of wave frequency data.



Figure 3.6: Wave maker



Figure 3.7: Frequency regulator

In this research solitary-like waves were produced that moves from wavemaker towards the end of the flume. To prevent waves from reflecting once they reach the end of the hydraulic flume, horsehair was positioned at the end of the Hydraulic Flume. When the waves reach the end of the channel, some of their water volume crosses the barrier and enters the container behind since most of these waves happen above the water's surface. The examination of the wave transmission coefficient and other physical variables might be greatly impacted by reflected waves from the barrier because of the relatively short hydraulic flume in this experiment. In order to overcome this, selective gauge measurements concentrating on determining transmission and reflection coefficients by utilizing the same time interval, or effective wave period were accounted. To lessen the impact of reflected waves on the outcomes, readings of water elevation fluctuation within a constant propagation were noted down prior to reflections. Wave height (H_i) generated in relation to their individual wave periods and depths are shown in Table 3.1.

Table 3.1: Wave heights in relation to wave period and depth

Wave Condition	Water Depth (m)	Wave Period T (s)	Wave Height Hi (m)
1	0.127	1.132	0.040
2	0.127	1	0.041
3	0.153	1.132	0.045
4	0.153	1	0.069
5	0.102	1.132	0.026
6	0.102	1	0.030
7	0.114	1.132	0.031
8	0.114	1	0.038

3.1.4 Image recording

Most of the data collection procedure comprised visual evaluations using scale positioning. To reduce mistakes, each assessment was repeated three times. However, a high-speed camera with a maximum frame rate of 24 frames per second, outfitted with Nikon 50 mm lenses, was also deployed to further reduce visual mistakes, validate readings, and allow cross-verification. The camera was positioned at the front of the hydraulic flume and runs the whole length of it. To ensure the necessary quality requirements were fulfilled, parameters including focus, aperture settings, and lighting conditions were carefully adjusted.

3.1.5 Breakwater Models

Two distinct breakwater models were used in a comparison study to see how successfully each model dispersed the energy of incoming waves. Finding out which breakwater had the best wave-dissipation capacity was the aim of the experiment. A number of crucial features are also compared and evaluated, in addition to how well the breakwaters dissipate waves. This study examined both the solid and perforated versions of the two breakwaters. There were comparisons between the two kinds of breakwaters in the performance evaluation. Similar parameters were employed in previous research to determine the percentages of perforation for the BWs [4]. Schematic diagram of each breakwater is provided below in Figure 3.8 & 3.9.

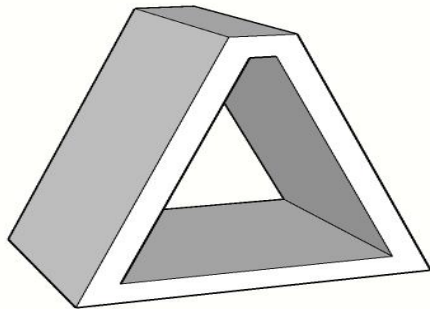


Figure 3.8: Triangular breakwater

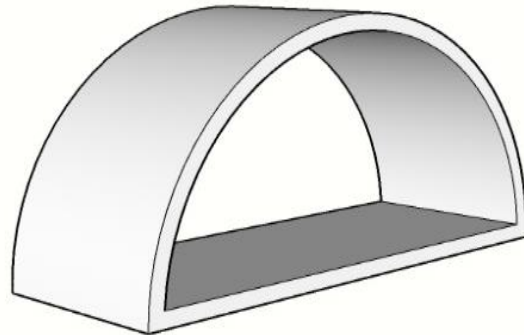


Figure 3.9: Semicircular breakwater

3.1.5.1 Triangular Breakwater (TBW)

The triangular form of the breakwater under consideration is what makes it unique. This subject study focused on assessing its performance in both a solid and a perforated condition. It was initially used in the Mekong River delta in a perforated shape. In present study, their performances were contrasted with one another. The breakwater was divided into four variations in a methodical manner. These variations consisted of one solid form and three other forms with different porosity percentages on the seaside and shoreside. The schematic diagram of permeable (perforated)

breakwater as well as the set of breakwaters used in current experimentation are shown in Figure 3.10 & 3.11. The accompanying Table 3.2 provides comprehensive details on different arrangements of the TBW.

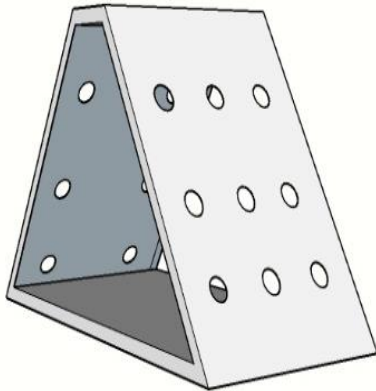


Figure 10: Permeable triangular breakwater



Figure 3.11: Real time triangular breakwater models

3.1.5.2 Semicircular Breakwater (SCBW)

Like TBW this SCBW was further subdivided into four different varieties, three of which are perforated and one of which is solid. Their schematic diagram as well as real time semicircular breakwater models are shown in Figure 3.12 & 3.13. As the Table 3.2 illustrates, their perforated shape has an equal % porosity to that of TBW.

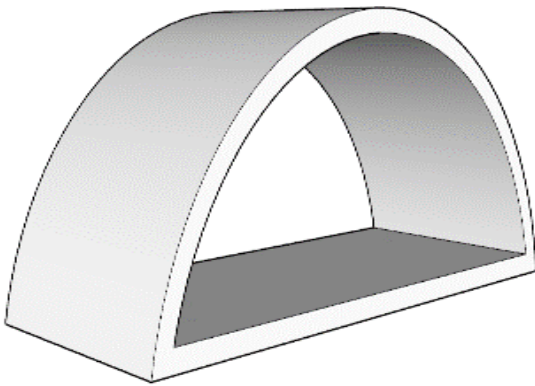


Figure 3.12: Permeable semicircular breakwater



Figure 3.13: Real time semicircular breakwater models

To ensure that breakwaters with comparable porosity levels may be fairly compared, this study maintains constant porosity percentages for each type of SCBW and TBW, classifying the numerous tests according to porosity for both the seaside and the shoreside. In addition, each breakwater's efficiency is evaluated independently within its own category to determine which breakwater porosity % is the best of its type, based on the percentage of perforation on both the seaside and the shoreside, Table 3.2 further divides each breakwater into four groups.

Table 3.2: Breakwater model types w.r.t porosities

BREAKWATER TYPE	SEASIDE		SHORE-SIDE	
	% Porosity	Diameter(cm ²)	% Porosity	Diameter(cm ²)
SC-1	Impermeable		Impermeable	
SC-2	36.60%	1.52	11.80%	0.991
SC-3	36.60%	1.52	22.50%	1.36
SC-4	10.80%	0.82	10.80%	0.82
TB-1	Impermeable		Impermeable	
TB-2	36.60%	1.67	11.80%	0.916
TB-3	36.60%	1.67	22.50%	1.31
TB-4	10.80%	0.82	10.80%	0.82

3.2 Measurement Techniques

The specified hydraulic boundary conditions, such as wave size and water depth, as well as the wave flume's ability to support the breakwater were considered while determining the physical model's dimensions. Froude's law was followed in the lab setting to ensure stable hydrodynamic conditions. The standards used to scale this model are the same ones that a researcher used in his research [4]. The following are the selected model scales.

Where Scale of length; $N_L = 30$

Table 3.3: Experimental model scales

Variables	Real Condition(m)	Flume capacity(m)	Scale
Max Water Depth	4	0.21	8
Max wave Height	1.5	0.042	35
Min water depth	1.4	0.026	54
Height of breakwater	3.3	0.114	29

There have been four variants tested for each of the two breakwaters in total. Physical conditions were kept consistent during the testing of these BWs. The same circumstances were applied to each BW during the examination: the same porosity percentages, the same depths, and the same wave periods. The shore was defined as the point where the hydraulic flume ends. It is important to clarify that when referring to both breakwaters having the same porosity, it actually signifies the percentage of porosity relative to their respective areas facing incoming waves and the outgoing waves.

Owing to the hydraulic flume's short length, there was a good chance that the waves produced by the wave generator would bounce when they reached the end, getting in the way of the ongoing measurements and observations. Following each reading, the wave-producing process was stopped and then restarted to reduce the possibility of interference from reflected waves. The thoughtful measurement and observation processes guaranteed an accurate and efficient data collection process. To guarantee the reliability and correctness of the data, each reading was recorded three times. The photographs during experimentation are shown in Figure 3.14 & 3.15.



Figure 3.14: Adjusting the frequency of Wave generator.



Figure 3.15: Horizontal as well as vertical scale with the help of which difference in wave parameters are quantified.

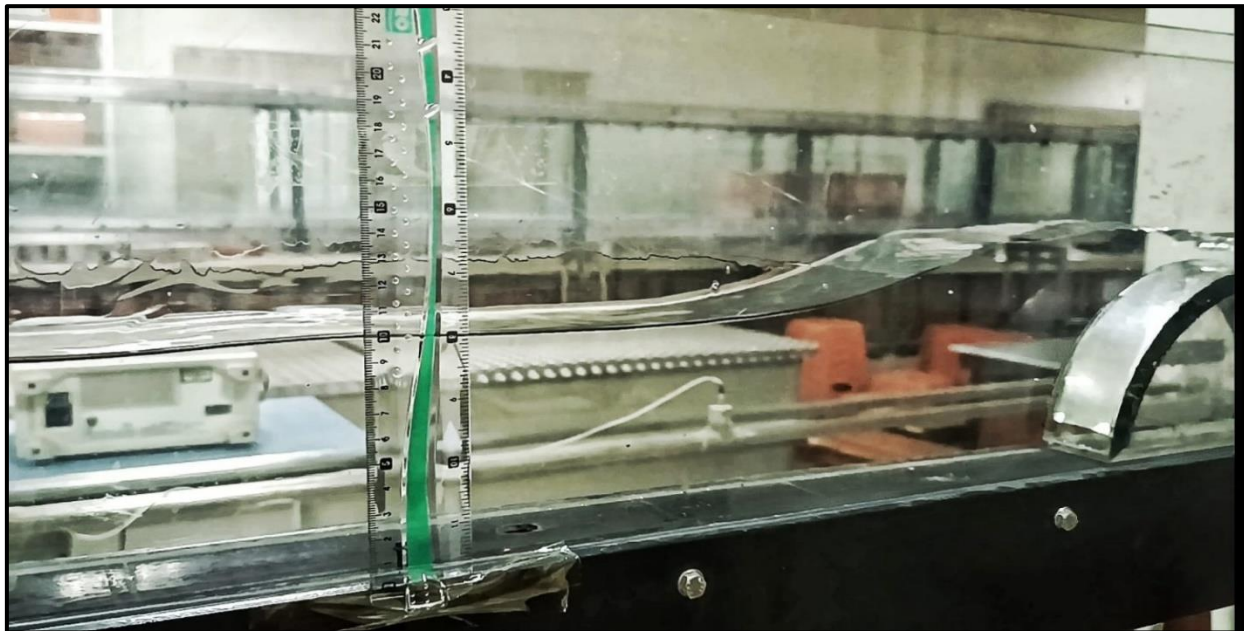


Figure 3.16: Incoming waves encountering Semicircular Breakwater (SCBW).

The waves generated by the wave generator are referred as incoming waves, and the letter H_i denotes their corresponding height. Once these waves hit the breakwater and rebound these waves are referred as reflected waves and their height is denoted as H_r . In the similar way, waves that have traveled through BW and been dispersed by the breakwater are referred to as transmitted waves and dissipated waves, respectively. These specific heights are indicated by the H_t and H_d , respectively.

Based on the experimental setup of Zelt [56] this experiment setup was made, SC-1 measures the height of incident waves (H_i), whereas SC-2 and SC-3 measure the height of reflected waves (H_r). With SC-4 and SC-5 were used to measure the height of transmitted waves (H_t). On the other hand, the difference between H_i and H_r was used to compute H_d height. But recording H_r proved especially difficult because of the interaction between incoming and reflected waves, which caused more and more disturbances with time. As a result, measurements of the same experiment were repeatedly carried out to guarantee the accuracy of the data. In order to get the most precise readings, camera video was also paused and played in slow motion to get the most precise results. It is important to note that higher frequencies of wave maker produce more heightened waves as compared to the waves produced at low frequency.

To find out how wave parameters affect wave-structure interaction, a total of 56 No. of experiments were carried out. Three categories were methodically created from the testing.

- Both Breakwaters (BW) were investigated in the first category in their solid form specifically impermeable state. These experiments were performed with a constant wave period of 1 and 1.132 seconds at depths of 0.127 m and 0.153 meters. The breakwaters were placed strategically 2.4 meters away from the shore.

- In the second category both impermeable and perforated forms of semicircular breakwaters (SCB) and triangle breakwaters (TB) were investigated. The experimental tests were carried out at a depth of 0.102 and 0.114 meters.
- Similarly in the third category two of the forms of breakwaters were evaluated at the same set wave period and depth. Their position from the coast was taken into consideration when evaluating their performance.

Previous research by [57] [58] has shown that a variety of characteristics significantly affect the wave's capacity to pass through breakwaters. These variables include wave qualities; significant wave height (H_s), wave period, and the unique design or shape of the breakwater, as well as freeboard (R_c) as well as the breakwater's inclined face slope, crest width (B), and surface porosity. To better understand their behavior, a new non-dimensional parameter was also introduced in this current study.

Since the crest width of the breakwater in the TBW was much less than the design wavelength, the crest width factor has not been taken into consideration. Furthermore, the effects of this parameter were not investigated in the conducted tests as the breakwater's slope does not change.

The total energy of the first wave generated was represented by the symbol E_i as it approaches the breakwater. When the energy encounters the breakwater, it splits into three sections. E_r is the amount of energy of waves that are reflected. When a portion of the wave successfully passes over the breakwater, it conveys energy known as transmitted wave energy, or E_t . Dissipated wave energy, represented by ϵ , is the total amount of energy lost during this process [59]. The law of conservation of energy theoretically derives equation (1) from the energy balance equation and can be written as:

$$E_i = E_r + E_t + \varepsilon \quad (3.1)$$

Where,

E_i = incoming wave energy

E_r = reflected wave energy

E_t = transmitted wave energy

ε = dissipated wave energy

$$\varepsilon = E_i - E_r - E_t \quad (3.2)$$

and so,

The energy balance formula can be rewritten as follows:

$$1 = K_t^2 + K_r^2 + K_d^2 \quad (3.3)$$

Where K_r is the Reflection Coefficient and is given as

$$K_r = H_r / H_i \quad (3.3.1)$$

K_t is the Transmission Coefficient which is given as

$$K_t = H_t / H_i \quad (3.3.2)$$

And the K_d is the dissipation coefficient which is found by finding the value of other two.

Using linear wave theory, as per wavelength, per unit crest width [60].

Where,

$$E_i = 1/8 \rho g (H_i)^2 \quad (3.4)$$

$$E_r = 1/8 \rho g (H_r)^2 \quad (3.5)$$

$$E_t = 1/8 \rho g (H_t)^2 \quad (3.6)$$

$$\varepsilon = 1/8 \rho g (H_i)^2 - 1/8 \rho g (H_r)^2 - 1/8 \rho g (H_t)^2 \quad (3.7)$$

$$\varepsilon / 1/8 \rho g (H_i)^2 = 1 - K_r^2 - K_t^2 \quad (3.8)$$

Chapter 4: RESULTS AND DISCUSSIONS

4.1 Impermeable Breakwaters

Both BWs in this subclass underwent extensive testing in their impermeable form. Breakwaters were tested in the presence of monochromatic waves. Breakwaters were placed strategically in this categorization with a separation of 2.4 meters from the shoreline. There were two different depths covered in this testing category. The tests were conducted here with the water level higher than BW height. Stated differently, BW was tested in this category as an immersed version. Waves were created at two distinct frequencies which resulted in the production of waves of different heights. As the accompanying Table 5.1 illustrates, waves produced at two frequencies and two depths resulted in a total of four different wave heights.

Every time, the created wave heights were a slightly different. To guarantee a thorough and efficient evaluation, each scenario was repeated three times, calculated the mean, and chose a particular reading for each test.

Regarding wave dissipation, all breakwaters performed admirably in case of waves dissipation as can be seen in Table 4.1. TBW demonstrated an interesting wave reflection phenomenon, in which a significant fraction of the wave reflected as it encountered the breakwater. As a result, there was a great deal of disruption which was clearly seen along the shore and ultimately resulted in larger K_r values as can be seen in the accompanying table.

Table 4.1: Wave dissipation percentages of both breakwater in impermeable form

Exp. No	# BW	Depth (m)	T(s)	λ (m)	H_i	H_r	H_t	H_s/L	K_r	K_t	K_d	E_i	E_r	E_t	ϵ	$\epsilon\%$
1	SCBW-1	0.127	1.13	0.47	0.040	0.011	0.009	0.171	0.287	0.231	0.930	1.936	0.159	0.104	1.673	86.42
2		0.127	1.00	0.44	0.041	0.014	0.012	0.186	0.332	0.283	0.900	2.059	0.227	0.165	1.668	80.99
3		0.153	1.13	0.51	0.045	0.017	0.015	0.174	0.386	0.333	0.860	2.459	0.367	0.272	1.820	74.03
4		0.153	1.00	0.48	0.069	0.032	0.028	0.285	0.466	0.408	0.785	5.782	1.254	0.960	3.567	61.69
5	TBW-1	0.127	1.13	0.47	0.040	0.016	0.013	0.171	0.403	0.334	0.852	1.936	0.314	0.216	1.406	72.65
6		0.127	1.00	0.44	0.041	0.021	0.018	0.186	0.512	0.434	0.741	2.059	0.540	0.388	1.131	54.92
7		0.153	1.13	0.51	0.045	0.025	0.021	0.174	0.558	0.478	0.679	2.459	0.766	0.561	1.132	46.04
8		0.153	1.00	0.48	0.069	0.041	0.036	0.285	0.603	0.524	0.602	5.782	2.100	1.588	2.094	36.23

When examining TBW separately, in Case 5, TBW yields maximum percentage dissipation and lowest K_r value as compared to the other 3 cases from Serial no 6 – 8. Since the incident wave height was lower than in the other three cases (6–8) as compared to case 5. Even the hydraulic jump forms on the seaside, just next to the BW's crest, in cases 7 and 8. Higher wave heights caused the BW's dissipation tendencies to decrease significantly, which caused a substantial quantity of the waves to cross the BW and raises height of reflected waves near the shore.

In case of SCBW, which performed marvelously in every scenario. Its percentage wave dissipation tendency was clearly greater than TBW which can be possibly due to its well-thought-out shape that has slopes on both sides. The breakwater effectively breaks up waves that are headed towards the SCBW, minimizing splashing and disturbances at the barrier. As can be witnessed from the Table 4.1 from serial number 1 to 4, the unique shape of the SCBW consistently generates lower K_r values in all four cases.

It is most critical to note that that the effectiveness of Breakwater may decrease as wave height increases above a certain limit and may fail after a certain threshold. In this particular study the wave heights examined in the current trials were less than that specific threshold.

Furthermore, it is important to mention that the approaching wave height in Case 1 was lower than in the other three situations of SCBW and same in the case of TBW. It's quite predictable that when waves of varying height hit breakwater of same type, less heighted H_i will produce least height of reflected waves and maximum wave dissipation percentages and vice versa which can also be observed from the Table 4.1.

The outcomes are quite surprising when the impermeable versions of the two breakwaters (BWs) were compared side by side with same incoming wave heights (H_i). In all four cases, SCBW performed noticeably better than TBW. When the height of the incoming wave increased, TBW

was able to counteract most of the waves with good performance, but the percentage of wave energy dissipation tendency decreased gradually. However, SCBW fared quite well in every situation, particularly when it came to producing very low heights of waves, which is important as in real world situations these higher reflected wave heights have the potential to seriously damage the shoreline and potentially erode the BW structure. Furthermore, the threshold for wave dissipation.

In terms of overall wave energy dissipation tendencies, SCBW-1 accomplished better than TBW-1, resulting in lower reflected wave heights and higher percentages of wave energy dissipation tendencies. As can be witnessed from the accompanying Table 4.1.

To get better understanding results of these experiments are shown in the graphical forms where H_s/L is place on X-axis and compared K_r , K_t and K_d of both SCBW-1 and TBW-1 individually.

Here,

$$H_s/L = \text{slope of wave}$$

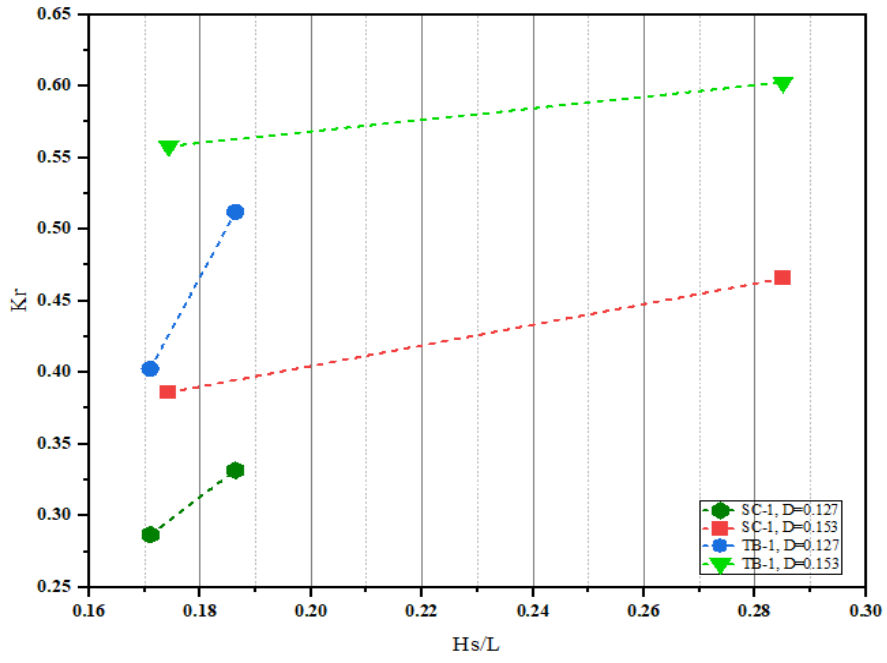


Figure 14: Coefficient of reflection

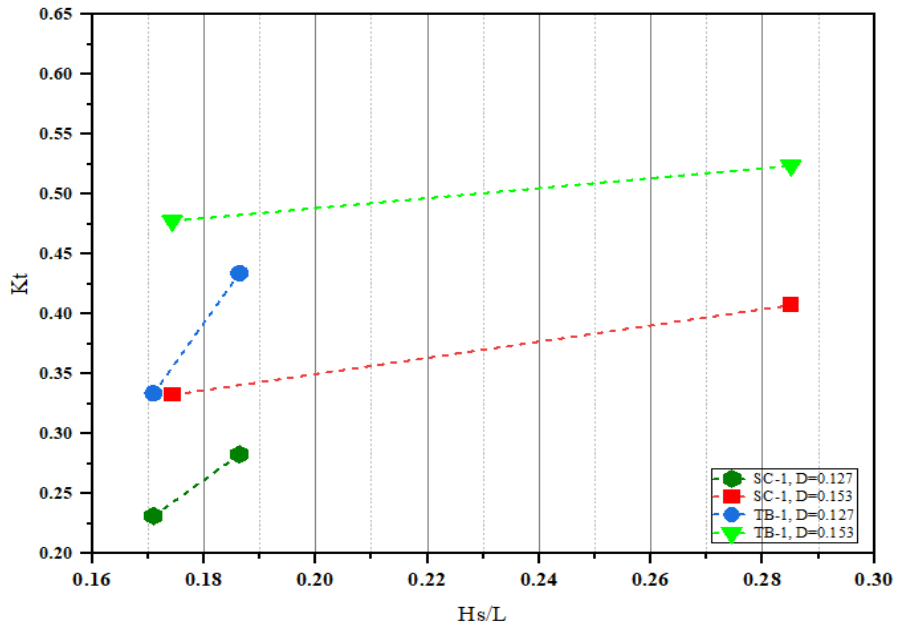


Figure 15 Coefficient of transmission.

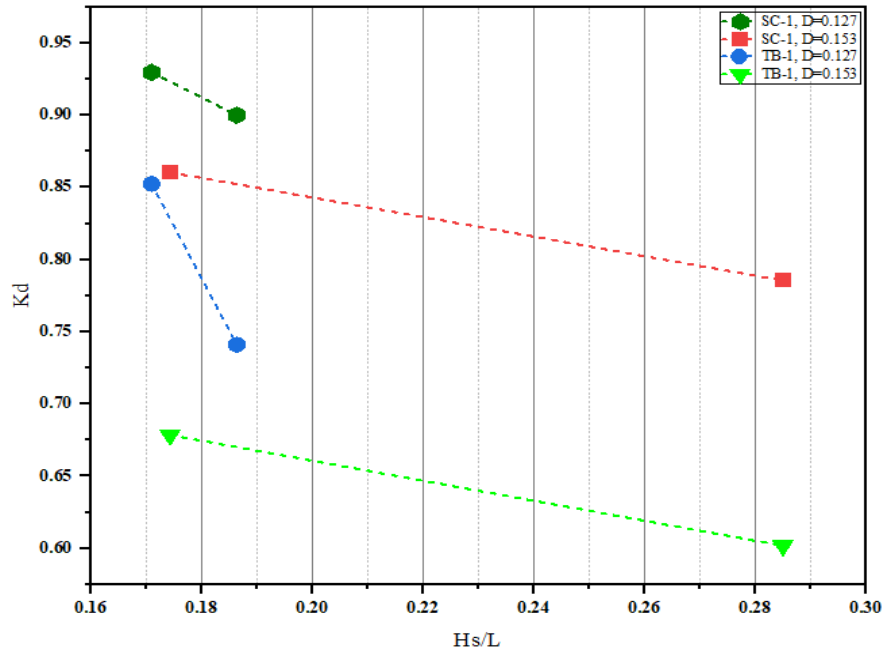


Figure 16 Coefficient of dissipation.

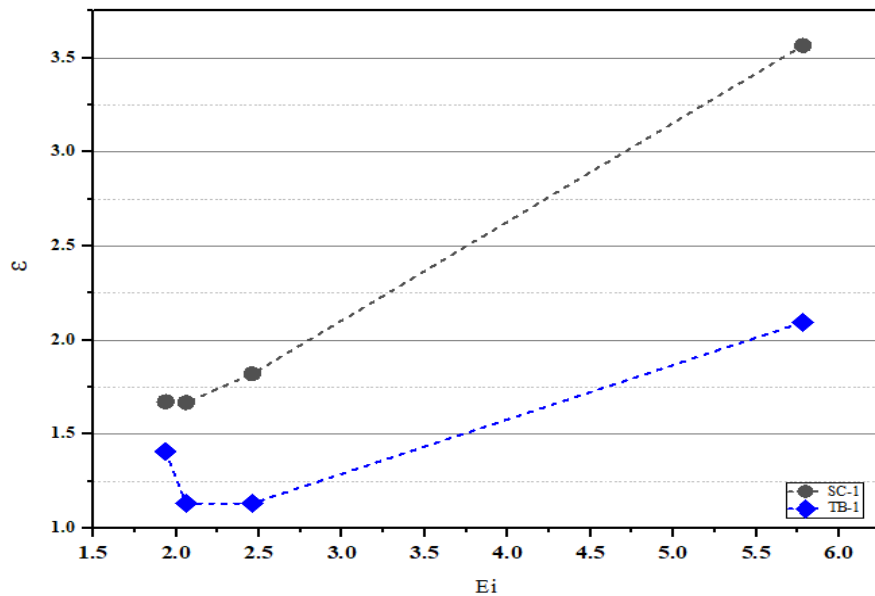


Figure 17 Relation of wave energy dissipation and incoming wave energy.

From the Figure 4.1, it is evident that SCBW-1 with red and dark green line exhibits the lowest K_r values in all scenarios compared to TBW-1 which is shown by the blue and the light green lines. Consequently, it demonstrated higher K_t values of SCBW-1 than TBW-1 in Figure 4.2. Despite this, due to its circular shape, SCBW-1 effectively mitigates incoming wave energy, resulting in

lower k_r values compared to TBW-1 as can be seen in Figure 4.3. The Figure 4.4 summarizes these findings by plotting dissipated wave energy on the Y-axis and Incoming wave energy (E) on X-axis for both types of BWs and it is clear from the figure, dissipation tendencies of SCBW are much higher than TBW.

4.2 Permeable Breakwaters

In this second stage of experimentation SCBW and TBW were tested in their permeable states. Each Breakwater (BW) in this context was tested in three different porosity situations. In line with the previous set of experimentation BW BW was situated 2.4 meters from the coast. This time, though, there were two distinct depths at which experiments are performed, in which the water depth at first was equal to the height of BW, and in the second there was a freeboard of 1 cm. These tests were run using the wave maker's two frequencies. As a result, the experiment produced four different values of H_i .

In this stage of testing three different porosities of both the breakwaters were placed together and they were tested individually side by side for better understanding and comparison of the dissipation tendencies of both the breakwaters in their different seaside and shoreside porosities to allow for a more detailed performance comparison.

4.2.1 SCBW-2 and TBW-2

First, SCBW-2 and TBW-2 were evaluated in this comparison research. Both had a porosity of 11.5% on the shore-side and 36.6% on the seaside. The examination results are displayed in the Table 4.2 at serial numbers 1- 4 for SCBW and 5-8 for TBW. Notably, the analysis showed that waves enter through the seaside openings and become caught inside the breakwater due to the shore side's decreased porosity, which limits the waves' ability to move through the breakwater.

Because of this constraint, more waves were reflected by Breakwater. More disturbance results from more waves striking the breakwater, which raised overall K_r values.

Nevertheless, a close examination of SCBW-2 on serial no 1- 4 and TBW-2 on serial no 5-8 results reveal that percentage dissipation of SCBW-2 were much better than TBW-2.

In addition to the comparison of wave energy dissipation of both the breakwaters in permeable form. In this category the impact of relative freeboard, which is indicated by Rc/H , on K_r , K_d and K_t of both the breakwaters was examined.

Here,

$$\text{Relative freeboard} = Rc/H$$

$$Rc = \text{freeboard above Breakwater}$$

$$H = \text{Average incoming wave height.}$$

Table 4.2: Wave dissipation percentages of Both Breakwater with seaside porosity of 36.6% and shoreside porosity of 11.8%.

Exp No.		Depth(m)	Rc	Rc/H	Distance from shore (m)	Seaside porosity (%)	Shoreside porosity (%)	F(Hz)	λ	Hi	Hr	Ht	Kr	Kt	Kd	Ei	Er	Et	ε	$\varepsilon\%$
1	SCB-2	0.102	0.013	0.488	3.5	36.6	11.8	0.883	0.410	0.026	0.011	0.003	0.437	0.131	0.890	0.828	0.158	0.014	0.66	79.20
2		0.102	0.013	0.431	3.5	36.6	11.8	1.000	0.398	0.030	0.014	0.005	0.466	0.154	0.871	1.066	0.232	0.025	0.81	75.90
3		0.114	0.000	0.000	3.5	36.6	11.8	0.883	0.435	0.031	0.015	0.006	0.487	0.182	0.854	1.192	0.283	0.039	0.87	72.96
4		0.114	0.000	0.000	3.5	36.6	11.8	1.000	0.420	0.038	0.020	0.008	0.523	0.219	0.824	1.741	0.475	0.083	1.18	67.92
5	TBW-2	0.102	0.013	0.488	3.5	36.6	11.8	0.883	0.410	0.026	0.012	0.004	0.467	0.150	0.872	0.828	0.180	0.019	0.63	75.98
6		0.102	0.013	0.431	3.5	36.6	11.8	1.000	0.398	0.030	0.015	0.005	0.505	0.183	0.843	1.066	0.272	0.036	0.76	71.14
7		0.114	0.000	0.000	3.5	36.6	11.8	0.883	0.435	0.031	0.017	0.007	0.529	0.220	0.820	1.192	0.334	0.058	0.80	67.20
8		0.114	0.000	0.000	3.5	36.6	11.8	1.000	0.420	0.038	0.021	0.009	0.562	0.251	0.788	1.741	0.551	0.109	1.08	62.09

The effects of relative freeboard on the K_r , K_d and K_t can be seen in the following Figures 4.5, 4.6 & 4.7.

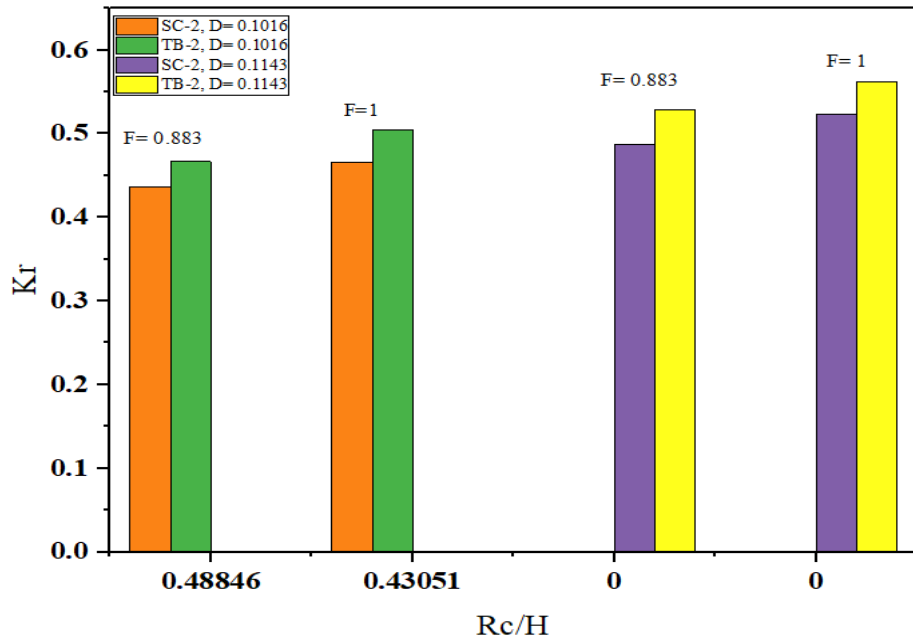


Figure 18 Relation btw Relative freeboard & Coefficient of reflection

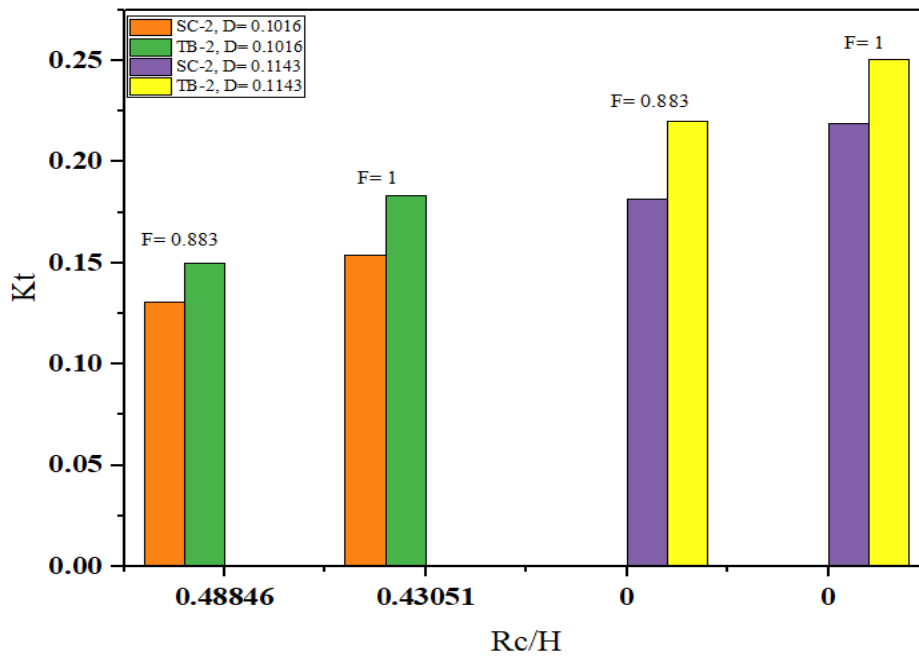


Figure 19 Relation btw Relative freeboard & Coefficient of Transmission

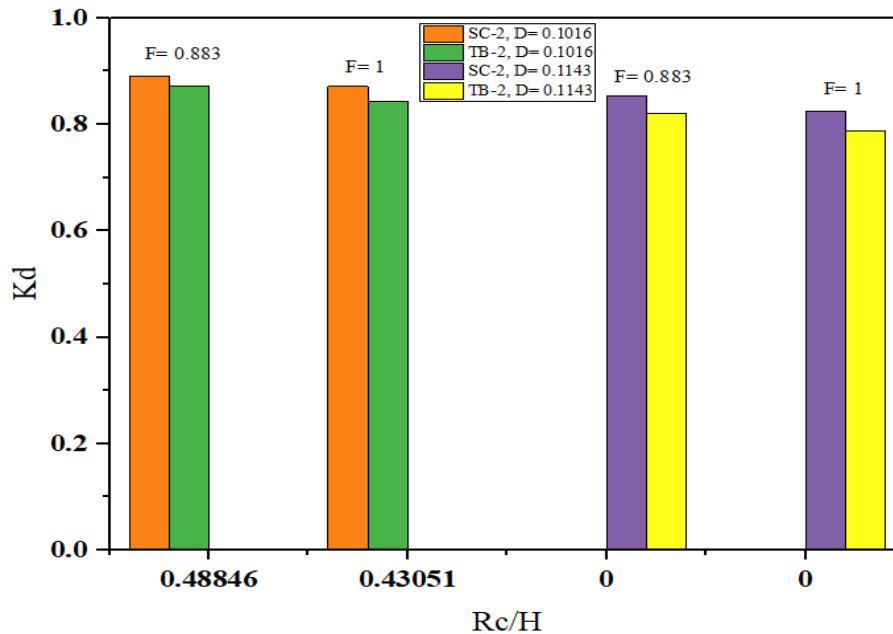


Figure 20: Relation btw Relative freeboard & coefficient of dissipation

According to the findings it is revealed that the relative freeboard is directly proportional to K_d as can be seen in Figure 4.7 and inversely proportional to K_r and K_t which can also be witnessed from Figure 4.5 & 4.6. Though, it is worth mentioning that as the relative freeboard decreases, the coefficient K_t will continue to be increasing, but in the case of K_r , it will start decreasing after reaching a certain edge. For K_d , R_c/H is directly proportional to K_d . In this case, K_d will also begin to decline as the sea depth significantly increases and wave heights surpass the breakwater's ability to tolerate and dissipate them.

4.2.2 SCB-3 and TBW-3

In this scenario SCBW-3 and TBW-3, with seaside porosities of 36.6% and 22.5% on the shore side for both BWs were compared. According to these findings, both breakwaters performed admirably. Waves pass through the breakwaters more easily because of the increased porosity on the seaside of TBW-3 and SCBW-3, which reduced wave reflection. Moreover, the elevated

porosity along the shoreline easily transfers waves, resulting in a relatively calm sea behind the breakwater.

The SCBW-3 instance exhibits very tiny heights of reflected waves as can be seen in Table 4.3, suggesting the best possible porosity on both the seaside and the shoreside. Additionally, each time a single wave strikes the breakwater, a vacuum-like cavity is created, giving incoming waves additional room to travel through the breakwater with ease. Two key components of this breakwater's unexpected efficiency regarding wave energy dissipation are its ideal porosity and the shape of SCBW which plays a critical role in reducing wave energy and preventing large disruptions from occurring in the area around the breakwater. Notably, as mentioned by researcher [4], the same percentage of porosity was thought to be ideal for optimizing wave dissipation and decreasing wave reflection.

However, TBW-3 also accomplished very well. But unlike SCBW-3, because of its sharply angled structure, it produced larger reflected waves, and more of the waves pass over the breakwater, creating a lot more disruption at the breakwater consequently resulted in decreased wave dissipation percentages as can be witnessed in the cases from Table 4.3 at serial no 5-8.

Table 4.3: Wave dissipation percentages of both breakwater with seaside porosity of 36.6% and shoreside porosity of 22.5%.

Exp No.		Depth (m)	Rc	Rc/H	Distance from shore. (m)	Seaside porosity (%)	Shoreside porosity (%)	F(Hz)	λ	Hi	Hr	Ht	Kr	Kt	Kd	Ei	Er	Et	ε	$\varepsilon\%$
1	SCBW-3	0.102	0.013	0.488	3.5	36.6	22.5	0.88	0.41	0.026	0.009	0.003	0.351	0.098	0.931	0.828	0.102	0.008	0.718	86.74
2		0.102	0.013	0.431	3.5	36.6	22.5	1.00	0.40	0.030	0.011	0.003	0.377	0.116	0.919	1.066	0.151	0.014	0.900	84.44
3		0.114	0.000	0.000	3.5	36.6	22.5	0.88	0.44	0.031	0.012	0.004	0.398	0.138	0.907	1.192	0.189	0.023	0.981	82.24
4		0.114	0.000	0.000	3.5	36.6	22.5	1.00	0.42	0.038	0.016	0.006	0.431	0.156	0.889	1.741	0.324	0.042	1.375	78.98
5	TBW-3	0.102	0.013	0.488	3.5	36.6	22.5	0.88	0.41	0.026	0.010	0.003	0.384	0.116	0.916	0.828	0.122	0.011	0.695	83.92
6		0.102	0.013	0.431	3.5	36.6	22.5	1.00	0.40	0.030	0.012	0.004	0.421	0.136	0.897	1.066	0.189	0.020	0.858	80.45
7		0.114	0.000	0.000	3.5	36.6	22.5	0.88	0.44	0.031	0.014	0.005	0.443	0.153	0.883	1.192	0.234	0.028	0.930	78.02
8		0.114	0.000	0.000	3.5	36.6	22.5	1.00	0.42	0.038	0.018	0.007	0.475	0.183	0.861	1.741	0.392	0.058	1.291	74.13

The co-relation of relative freeboard and the respective K_r , K_d and K_t for both types of BW's are given below in Figure 4.8 to 4.10.

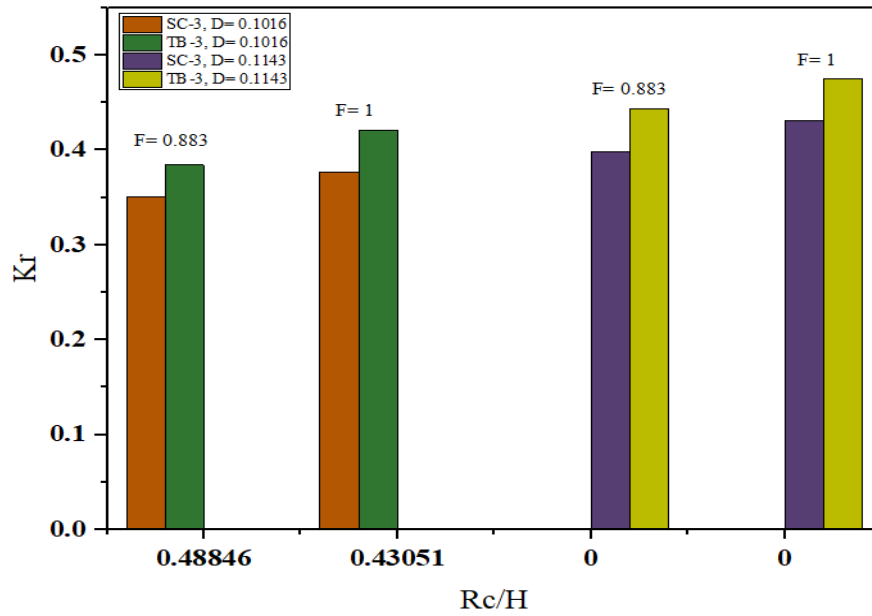


Figure 21: Relation btw Relative freeboard & Coefficient of reflection

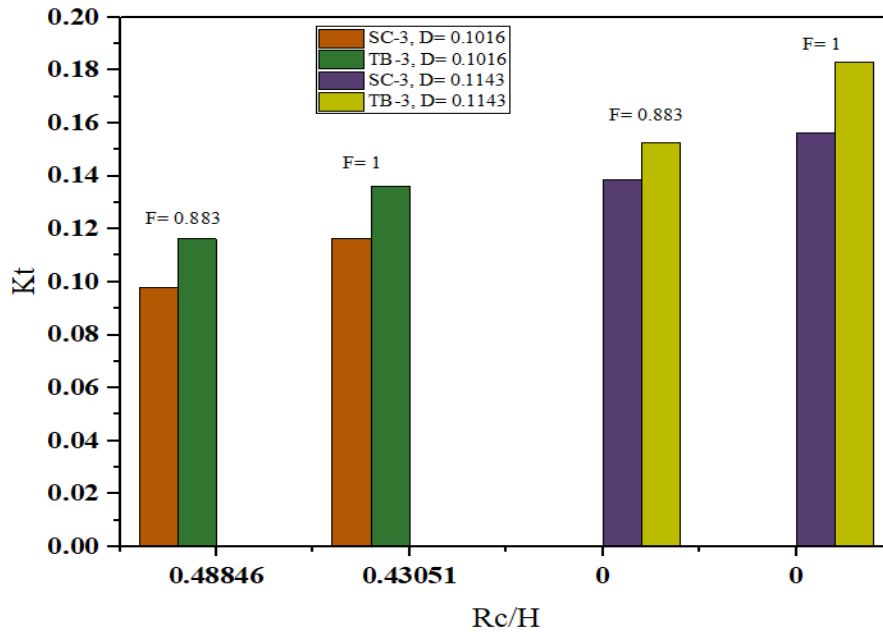


Figure 22: Relation btw relative freeboard & coefficient of transmission

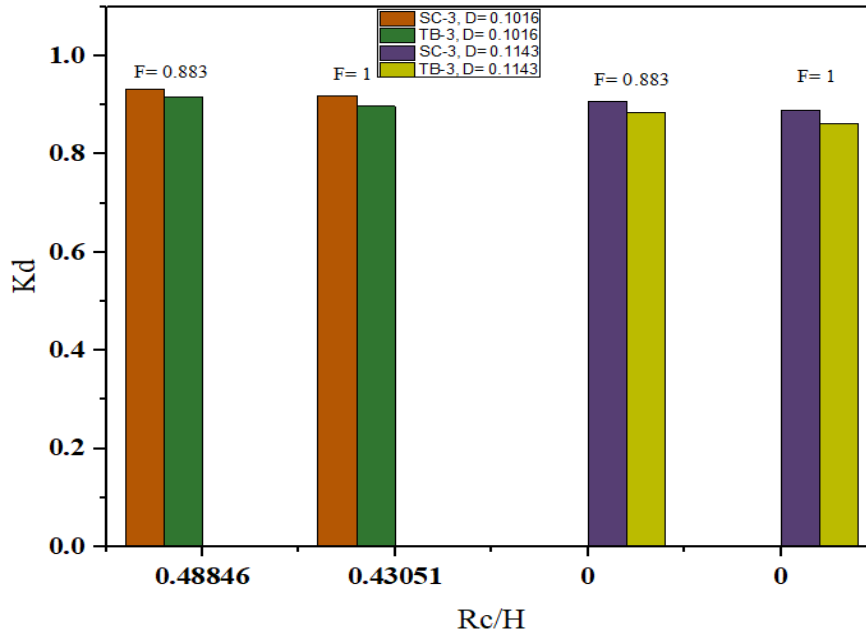


Figure 23: Relation btw relative freeboard & coefficient of dissipation

4.2.3 SCB-4 and TBW-4

Within the context of SCBW-4 and TBW-4, where the porosity of both breakwaters is the same (10.8% on the seaside and shoreside), higher reflected waves were observed, which lead to higher K_r values because of wave reflection. As the Table 4.4 plainly illustrates, lower K_t values for both BW's due to increased wave reflection resulting in larger values of K_r and consequently lower percentages of wave dissipation overall.

In this case as the porosity percentage is the same on the seaside as well as on the shoreside, higher values of K_r and particularly K_t were observed. It's crucial to remember that SCBW-4 outperformed TBW-4 in comparison which can be observed from the percentage dissipation tendencies of both the breakwaters in the accompanying Table 4.4, the wave dissipation percentages of SCBW-4 which is at serial no 1-4 and with that of TBW-4 whose are at serial no 5-8 are matched. Measuring the height of the reflected wave in the case of TBW-4 became extremely challenging due to the high wave distortions.

Table 4.4: Wave dissipation percentages of both breakwater with seaside porosity and shoreside porosity of 10.8%.

Exp No.		Depth(m)	Rc	Rc/H	Distance from shore. (m)	Seaside porosity (%)	Shoreside porosity (%)	F(Hz)	λ (m)	Hi	Hr	Ht	Kr	Kt	Kd	Ei	Er	Et	ϵ	$\epsilon\%$
1	SCBW-4	0.102	0.013	0.488	3.5	10.8	10.8	0.883	0.410	0.026	0.013	0.005	0.512	0.192	0.837	0.828	0.217	0.031	0.581	70.1
2		0.102	0.013	0.431	3.5	10.8	10.8	1.000	0.398	0.030	0.016	0.007	0.536	0.227	0.813	1.066	0.306	0.055	0.705	66.2
3		0.114	0.000	0.000	3.5	10.8	10.8	0.883	0.435	0.031	0.018	0.008	0.564	0.253	0.786	1.192	0.379	0.076	0.737	61.8
4		0.114	0.000	0.000	3.5	10.8	10.8	1.000	0.420	0.038	0.022	0.011	0.581	0.289	0.761	1.741	0.588	0.146	1.008	57.9
5	TBW-4	0.102	0.013	0.488	3.5	10.8	10.8	0.883	0.410	0.026	0.014	0.006	0.535	0.235	0.812	0.828	0.237	0.046	0.546	65.9
6		0.102	0.013	0.431	3.5	10.8	10.8	1.000	0.398	0.030	0.017	0.008	0.569	0.258	0.781	1.066	0.346	0.071	0.650	60.9
7		0.114	0.000	0.000	3.5	10.8	10.8	0.883	0.435	0.031	0.019	0.009	0.609	0.287	0.740	1.192	0.442	0.098	0.652	54.7
8		0.114	0.000	0.000	3.5	10.8	10.8	1.000	0.420	0.038	0.024	0.013	0.645	0.350	0.679	1.741	0.725	0.213	0.803	46.1

The Figures 4.11 to 4.13 showing the relationship between the relative freeboard and the corresponding K_r , K_d , and K_t of SCBW-4 and TBW-4. are given below,

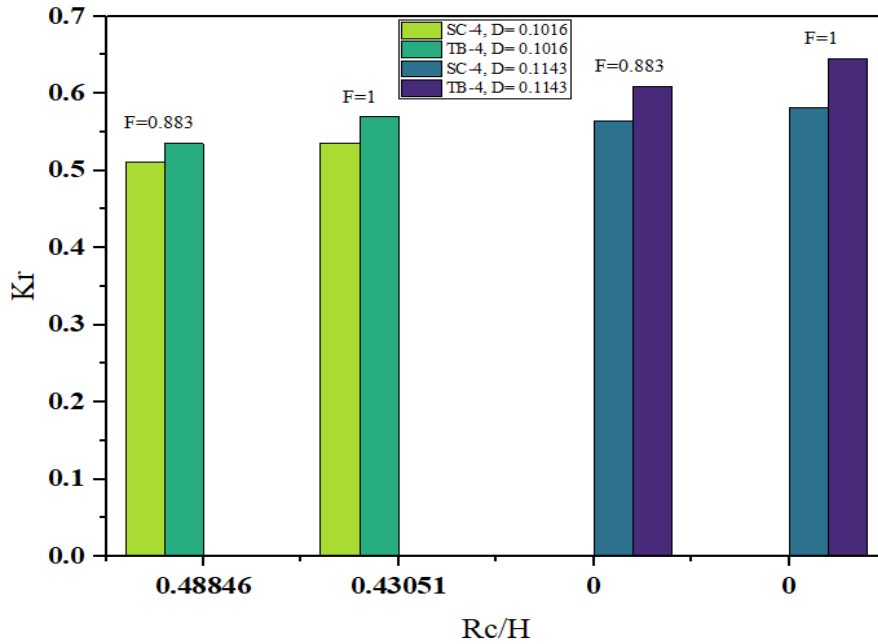


Figure 24: Relation btw relative freeboard & coefficient of reflection

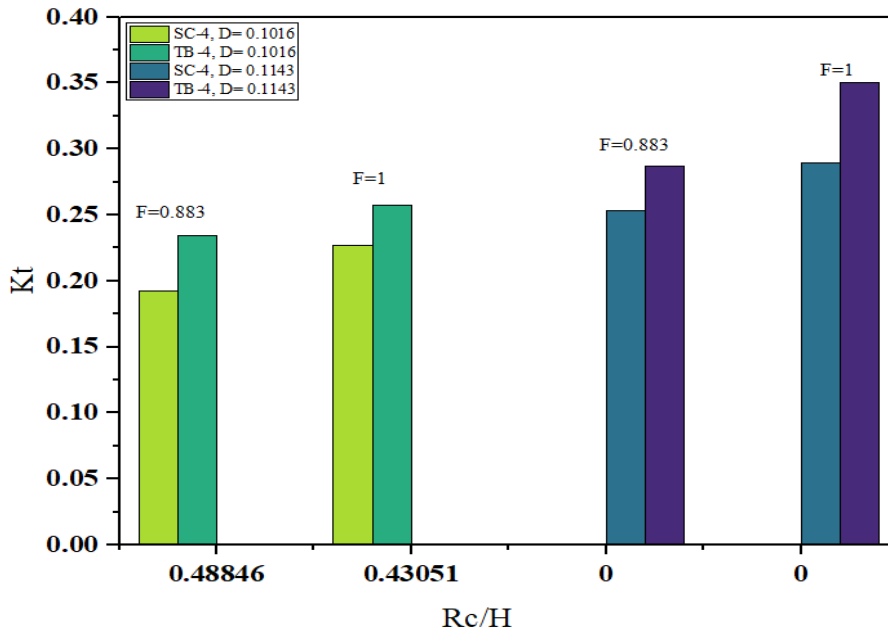


Figure 25: Relation btw relative freeboard & coefficient of transmission

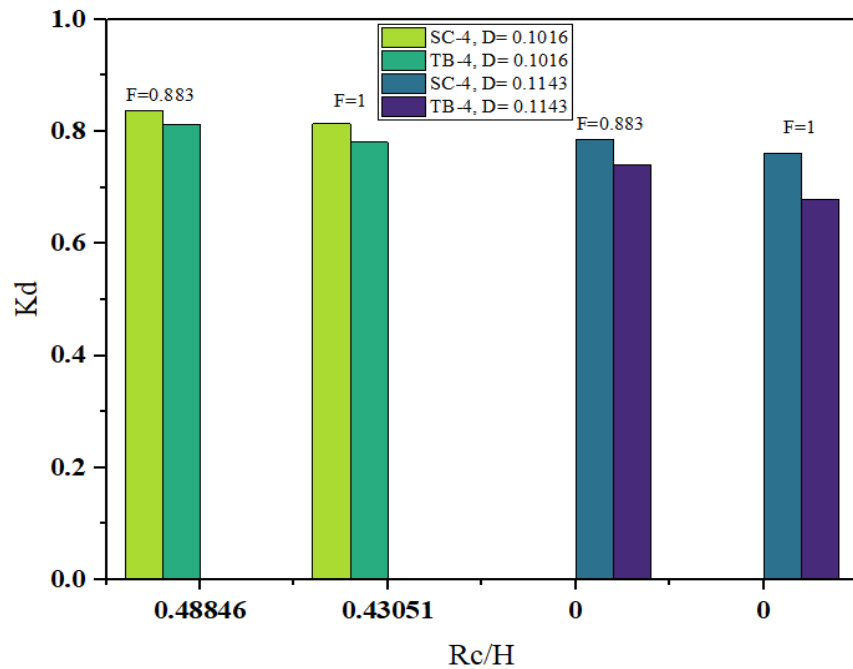


Figure 26: Relation btw relative freeboard & coefficient of dissipation

4.3 Summary of Results

The results show how well SCBW performed compared to TBW in the same wave height and depth conditions. Significant differences in percentage dissipation were detected while comparing SCB-2 and TBW-2, SCB-3 and SCB-3, and SCB-4 and TBW-4 in detail. Notably, SCBW consistently achieved lower values of K_r in nearly all cases, outperforming TBW not just in wave dissipation but also in other areas, maintaining tranquil environment behind breakwater. These lower K_r values are significant because they can reduce sea disturbances, which lessens potential difficulties for marine transportation.

In another scenario of these sets of experiments it is revealed that the relative freeboard is inversely proportional to K_r and K_t and directly proportional to K_d for breakwaters (up to a certain limit of

Rc/H). which means relative freeboard directly impact percentage wave energy dissipation. The dissipation percentage increases with increasing Rc/H value.

Upon comparing three different types of perforation scenarios within each type of breakwater, SCBW-3 exhibits the best performance in terms of wave dissipation and lower values of the reflection coefficient, causing very little disturbance along the shore side. Its sea-side porosity is 36.6%, while on the shore side it is 22.55%. Comparably, out of the two breakwaters in TBW with varying porosity situations, TBW-3 fared extremely well. Since it yields the lowest value of K_r and the highest value of % dissipation within its own type. So after all these results it was concluded that this porosity percentage is ideal among these porosity percentages.

Regarding the relationship of freeboard with reflection, transmission, and dissipation coefficients, it is revealed that the value of relative freeboard is directly proportional to the dissipation coefficient and inversely proportional to the reflection coefficient and transmission coefficient.

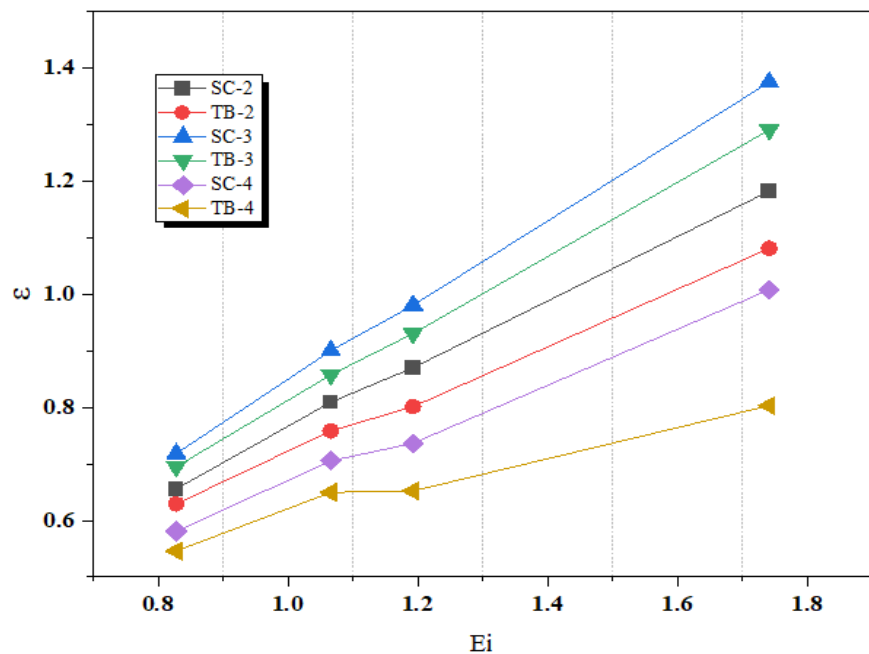


Figure 27: Relation btw dissipated wave energy & incoming wave energy

In this above Figure 4.14, the entire set of tests performed in our second category of experiments are shortened. It demonstrates the contrast of wave energy dissipation tendencies between SCBW and TBW across three different seaside and shoreside porosity conditions. The figure is plotted between dissipated wave energy and incoming wave energy. It precises the complete set of experiments and illustrate that SCBW has exceeded TBW in terms of wave dissipation. Furthermore, the figure highlights that SCBW-3 and TBW-3 display the highest wave energy dissipation tendencies among the other BWs of both categories which can be witnessed from the figure.

A number of experiments have confirmed and reinforced this observation, showing that the ideal conditions for maximizing wave energy dissipation tendencies and minimizing the height of reflected wave that is only possible by maintaining a calm shore behind the breakwater which was only possible by both the Breakwaters with the porosity of 36.6% on the seaside and 22.5% on the shore side.

4.4 Effect of Position of Breakwater on Wave Dissipation Tendencies

In this third testing phase, after determining the ideal BW and the optimal porosity percentage, the impact of shifting the breakwater's location with respect to shore on its ability to dissipate waves was inspected. In order to do this, all the four forms of two breakwaters in nine distinct locations in relation to the shore were positioned, beginning at 2.972 meters from the shore and progressively reducing the BW's distance from the shore to 1.422 meters. Each breakwater was tested at the same locations and at the same distance. The whole testing scenario in this category revolved around the placement of the BW to achieve the highest possible wave energy dissipation and the lowest possible wave reflection. to avoid interfering with sea transportation and harbor activities, operations or any other activities taking place along the seashore.

The water depth in this testing series was maintained at 0.114m, which was nearly equivalent to the BW height under test. Waves with a wavelength of around 0.435 meters were generated at a frequency of 0.883 Hertz, which nearly results in an average H_i of 0.034. Each breakwater was independently tested in nine distinct locations in relation to the coastline. This allowed us to analyze the dissipation tendencies of various BWs without freeboard and determine the optimal BW position in relation to the shore to achieve both maximal wave energy dissipation and a calm sea.

A new non-dimensional variable, the Shoreline Elevation Index (SEI), Z/L_s , was added to this specific category of experimentation.

Where,

$Z = \text{Height of Breakwater}$

$L_s = \text{Distance of BW from the shore.}$

The results of the experiments of all the BWs under experimentation are summarized in the Table 4.5 to 4.12.

Table 4.5: Relation of wave attenuation tendencies with location of breakwater for impermeable SCBW-1

SC-1								
Sr. No	Ls	Seaside porosity	Shoreside porosity	Z/Ls	Kr	Kt	Kd	$\epsilon\%$
1	2.972	Nill (solid)	Nill (solid)	0.03419149	0.354	0.212	0.921	83.0712716
2	2.839			0.03579198	0.367	0.225	0.903	81.5132872
3	2.706			0.03754966	0.384	0.232	0.894	79.8857353
4	2.573			0.0394889	0.396	0.244	0.884	78.1886159
5	2.440			0.04163934	0.411	0.254	0.874	76.4219291
6	2.186			0.04648822	0.442	0.267	0.856	73.3097232
7	1.931			0.05261523	0.473	0.281	0.837	69.998192
8	1.677			0.06060245	0.501	0.272	0.815	66.4873356
9	1.422			0.07144866	0.529	0.381	0.754	56.6704152

Table 4.6: Relation of wave attenuation tendencies with location of breakwater for SCBW-2

SC-2								
Sr. No	Ls	Seaside porosity (%)	Shoreside porosity (%)	Z/Ls	Kr	Kt	Kd	$\epsilon\%$
1	2.972	36.6	11.8	0.034191	0.2647	0.147	0.953	90.83901
2	2.839			0.035792	0.2862	0.158	0.944	89.31293
3	2.706			0.03755	0.3075	0.17	0.936	87.66931
4	2.573			0.039489	0.3289	0.181	0.926	85.90814
5	2.440			0.041639	0.3503	0.192	0.915	84.02944
6	2.186			0.046488	0.3658	0.215	0.906	82.01297
7	1.931			0.052615	0.3815	0.239	0.894	79.84802
8	1.677			0.060602	0.3964	0.262	0.883	77.53458
9	1.422			0.071449	0.4119	0.282	0.866	75.07266

Table 5: Relation of wave attenuation tendencies with location of breakwater for SCBW-3

SC-3								
Sr. No	Ls	Seaside porosity (%)	Shoreside porosity (%)	Z/Ls	Kr	Kt	Kd	$\epsilon\%$
1	2.972	36.6	22.5	0.034191	0.1765	0.058	0.983	96.544
2	2.839			0.035792	0.1973	0.073	0.977	95.583
3	2.706			0.03755	0.2176	0.089	0.972	94.495
4	2.573			0.039489	0.2382	0.102	0.965	93.280
5	2.440			0.041639	0.2589	0.111	0.959	91.938
6	2.186			0.046488	0.2694	0.127	0.956	91.098
7	1.931			0.052615	0.2807	0.136	0.952	90.212
8	1.677			0.060602	0.2919	0.148	0.945	89.279
9	1.422			0.071449	0.3025	0.158	0.941	88.300

Table 6: Relation of wave attenuation tendencies with location of breakwater for SCBW-4

SC-4								
Sr. No	Ls	Seaside porosity (%)	Shoreside porosity (%)	Z/Ls	Kr	Kt	Kd	$\epsilon\%$
1	2.972	10.8	10.8	0.034191	0.3001	0.173	0.937	87.999
2	2.839			0.035792	0.3191	0.186	0.929	86.353
3	2.706			0.03755	0.3383	0.199	0.920	84.601
4	2.573			0.039489	0.3575	0.213	0.911	82.742
5	2.440			0.041639	0.3764	0.225	0.899	80.778
6	2.186			0.046488	0.3993	0.247	0.885	77.911
7	1.931			0.052615	0.4222	0.271	0.865	74.833
8	1.677			0.060602	0.4449	0.294	0.847	71.543
9	1.422			0.071449	0.4676	0.319	0.824	68.041

Table 7: Relation of wave attenuation tendencies with location of breakwater for impermeable TBW-1

TBW-1								
Sr. No	Ls	Seaside porosity (%)	Shoreside porosity (%)	Z/Ls	Kr	Kt	Kd	ε%
1	2.972	Nill (solid)	Nill (solid)	0.034191	0.5646	0.353	0.745	55.633
2	2.839			0.035792	0.5793	0.375	0.724	52.468
3	2.706			0.03755	0.5941	0.394	0.701	49.175
4	2.573			0.039489	0.6086	0.415	0.676	45.756
5	2.440			0.041639	0.6232	0.436	0.651	42.210
6	2.186			0.046488	0.6481	0.463	0.603	36.262
7	1.931			0.052615	0.6729	0.497	0.548	30.000
8	1.677			0.060602	0.6978	0.529	0.484	23.422
9	1.422			0.071449	0.7226	0.559	0.408	16.530

Table 8 Relation of wave attenuation tendencies with location of breakwater for TBW-2

TBW-2								
Sr. No	Ls	Seaside porosity (%)	Shoreside porosity (%)	Z/Ls	Kr	Kt	Kd	ε%
1	2.972	36.6	11.8	0.034191	0.3824	0.205	0.901	81.166
2	2.839			0.035792	0.4183	0.228	0.879	77.332
3	2.706			0.03755	0.4543	0.249	0.856	73.142
4	2.573			0.039489	0.4902	0.273	0.828	68.596
5	2.440			0.041639	0.5262	0.294	0.798	63.694
6	2.186			0.046488	0.5445	0.327	0.773	59.647
7	1.931			0.052615	0.5623	0.362	0.744	55.303
8	1.677			0.060602	0.5802	0.397	0.715	50.661
9	1.422			0.071449	0.5983	0.430	0.676	45.721

Table 9 Relation of wave attenuation tendencies with location of breakwater for TBW-3

TBW-3								
Sr. No	Ls	Seaside porosity (%)	Shoreside porosity (%)	Z/Ls	Kr	Kt	Kd	$\epsilon\%$
1	2.972	36.6	22.5	0.034191	0.2909	0.132	0.948	89.806
2	2.839			0.035792	0.3035	0.144	0.943	88.753
3	2.706			0.03755	0.3160	0.154	0.936	87.644
4	2.573			0.039489	0.3286	0.155	0.934	86.833
5	2.440			0.041639	0.3412	0.176	0.923	85.256
6	2.186			0.046488	0.3585	0.191	0.915	83.534
7	1.931			0.052615	0.3758	0.205	0.904	81.714
8	1.677			0.060602	0.3932	0.219	0.895	79.794
9	1.422			0.071449	0.4105	0.232	0.882	77.776

Table 10 Relation of wave attenuation tendencies with location of breakwater for TBW-4

TBW-4								
Sr. No	Ls	Seaside porosity (%)	Shoreside porosity (%)	Z/Ls	Kr	Kt	Kd	$\epsilon\%$
1	2.972	10.8	10.8	0.034191	0.4698	0.237	0.850	72.318
2	2.839			0.035792	0.4919	0.269	0.829	68.645
3	2.706			0.03755	0.5141	0.298	0.804	64.688
4	2.573			0.039489	0.5363	0.329	0.778	60.447
5	2.440			0.041639	0.5586	0.359	0.747	55.920
6	2.186			0.046488	0.5747	0.386	0.722	52.167
7	1.931			0.052615	0.5911	0.410	0.695	48.229
8	1.677			0.060602	0.6073	0.437	0.664	44.106
9	1.422			0.071449	0.6235	0.462	0.631	39.798

The testing findings showed that the Semicircular Breakwater (SCBW) and the Triangular Breakwater (TBW) both exhibit a similar pattern of wave dissipation. But it's clear that in every test SCBW outperform TBW. Throughout these trials, SCBW's supremacy repeatedly observed. Additionally, it is clear from analyzing the effects of various porosity scenarios from Table 4.5 to 5.11 that the scenario with 36.5% porosity on the shoreside and 22.5% porosity on the seaside which are given in table 4.7 & 4.11 consistently performs better than all other porosity configurations for both types of breakwaters. In every test that was carried out, this ideal porosity configuration shows enhanced wave dissipation capabilities.

These findings of the dominance of SCBW and the identified optimal porosity scenario highlights the validity of previous tests performed. Evaluating the effectiveness of both types of breakwaters (BW) in relation to their distance from the shore is the main objective of this testing category. The idea was to see how the breakwaters' ability to dissipate waves changed with distance from the shore.

The wave dissipation tendencies of both types of breakwaters steadily declined when they were positioned closer to the shore, according to experiments conducted under fixed physical circumstances as can be witnessed from all the tables. To put it another way, the breakwaters capacity to dissipate waves energy diminished as the distance between BW and the shore decreases. This pattern can be observed in each Table from 4.5 to 4.12 that wave dissipation tendencies gradually decreases as breakwater is gradually moved from position 2.972 m from shore to the nearest point of the shore 1.422 m.

This pattern held true for every test instance and showed a direct correlation between the breakwaters ability to dissipate waves and their distance from the coast. It is crucial to give careful thought to where to place breakwaters in coastal protection plans, as evidenced by the observed

decline in wave dissipation tendencies when the breakwaters were positioned closer to the shore. These results offer important new information for placing breakwaters optimally to reduce the negative effects of waves on coastal regions. A significant finding emerges when phenomena of breakwaters' (BW) was examined diminishing wave dissipation tendency in relation to their decreasing distance from the beach; the height of incoming waves that reach the BW rises as the BW was positioned closer to the shore. This mimics the dynamics seen in actual maritime circumstances, where waves generally get higher as they go closer to the coast. But this rise in wave height is not a straight line; rather, it is impacted by the intricate relationship that exists between the waves and the ocean floor [61].

Incoming wave heights were measured using Scale SC-2 and initially see a constant height in experimental model where waves were generated at a given frequency and depth. But these waves start to get taller as they approach the BW. As the BWs were moved closer to the coast, this pattern keeps repeating. Higher reflected wave heights resulted from higher incoming wave heights. Furthermore, part of the wave topples the BW structure since more concentrated wave energy was present. As, the BW gets closer to the beach, causing both overtopping and enhanced reflection to happen more frequently.

The combined effect of these dynamics was a decrease in the BW's tendency towards wave dissipation. In essence, more of the incoming wave height is reflected and less was absorbed or dispersed by the BW structure when incident wave height rises as a result of the BW's close proximity to the coast. This demonstrated the intricate relationship that existed between breakwater location and wave dynamics, highlighting the significance of giving coastal engineering and protection methods serious thought. The findings from the above tables clearly demonstrate that farthest point from the shore at 2.972 meters, is the point at which maximal wave dissipation

occurred. In real world situations Breakwaters can't be positioned too far from the coast, either as this placement may interfere with maritime activities. Summarizing the above discussion, it was concluded that maximum wave attenuation results are obtained when breakwater models are placed farthest from the shore, moreover percentage wave dissipation tendencies depreciated as breakwater is placed close to the shore.

4.4.1 Statistical Analysis

A new non-dimensional variable Shoreline elevation Index (SEI), Z/Ls was added to this above category of experimentation, as previously specified. Therefore, how considerable wave dissipation tendencies depended upon this new non-dimensional variable was examined statistically. IBM SPSS Statistics 26 was used to build a linear regression model to examine the relationship between Z/Ls and wave dissipation tendencies. Here,

Here Z/Ls = Independent variable

Whereas,

Wave dissipation tendencies in the form of percentage of wave dissipation is taken as dependent variable.

$\epsilon\%$ = Dependent variable.

By using data of SEI and $\epsilon\%$ from Table 4.5 to 4.12 we run this model and these given below are the indicators to validate and check how dependent percentage dissipation is on newly introduced non dimensional parameter Shoreline elevation Index (SEI), Z/Ls .

4.4.1.1 R-square

In this case, the Shoreline Elevation Index (SEI), the independent variable, and the percentage dissipation tendency (ϵ) of the breakwaters (BW), the dependent variable, were assessed using the

crucial metric R-square. The value of R square truly indicates in percentage the extent to which the dependent variable actually depends on the independent variable. In other words, the total variation in dependent variable due to independent variable. The results of this metric are shown in the Table 4.13 to 4.20.

Table 11 R square for SCBW-1

R	(R) Square	Adapted R Square	Average Estimate Error
.994 ^a	.989	.987	.95031

Table 12: R square for SCBW-2

R	(R) Square	Adapted R Square	Average Estimate Error
.964 ^a	.929	.919	1.53633

Table 13 R square for SCBW-3

R	(R) Square	Adapted R Square	Average Estimate Error
.923 ^a	.852	.831	1.17728

Table 14 R square for SCBW-4

R	(R) Square	Adapted R Square	Average Estimate Error
.980 ^a	.959	.954	1.47586

Table 15 R square for TBW-1

R	(R) Square	Adapted R Square	Average Estimate Error
.982 ^a	.965	.959	2.71444

Table 16 R square for TBW-2

R	(R) Square	Adapted R Square	Average Estimate Error
.946 ^a	.896	.881	4.20307

Table 17R square for TBW-3

R	(R) Square	Adapted R Square	Average Estimate Error
.977 ^a	.954	.947	.95695

Table 4.18R square for TBW-4

R	(R) Square	Adapted R Square	Average Estimate Error
.942 ^a	.887	.871	4.01447

It is clear from looking at the tables above that the R-square values for the Triangular Breakwaters (TBW) and Semicircular Breakwaters (SCBW) are regularly higher than 0.8. With over 80% and perhaps up to 90% of the variance in the percentage dissipation tendency of the BWs, this indicates that independent variable, the SEI, has a significant impact on the dependent variable.

This high explanatory power suggests a considerable correlation between the breakwaters' dissipation tendencies and the shoreline elevation index. It emphasizes how important SEI is as a predictive variable for figuring out how well breakwaters will work to reduce wave energy in coastal locations.

4.4.1.2 ANOVA table

This ANOVA table was ran in order to predict the fitness of the regression model. Here if significant level is less than 0.05, it can be said that the relation between dependent and independent variable is significant. Here Significant level is often denoted by P-value. By

establishing the degree of significance. It is necessary to evaluate how the relation between dependent variable and the independent variable is significant.

Table 4.19 ANOVA results for SCBW-1

ANOVA (SCBW-1)						
Model		Sum of Squares	df	Mean Square	F	Sig.
1	Regression	563.691	1	563.691	624.185	.000 ^b
	Residual	6.322	7	.903		
	Total	570.012	8			
a. Dependent Variable: ε						
b. Predictors: (Constant), SEI						

Table 20 ANOVA results for SCBW-2

ANOVA (SCBW-2)						
Model		Sum of Squares	df	Mean Square	F	Sig.
1	Regression	216.687	1	216.687	91.805	.000 ^b
	Residual	16.522	7	2.360		
	Total	233.210	8			
a. Dependent Variable: ε						
b. Predictors: (Constant), SEI						

Table 4.21: ANOVA results for SCBW-3

ANOVA (SCBW-3)						
Model		Sum of Squares	df	Mean Square	F	Sig.
1	Regression	55.928	1	55.928	40.353	.000 ^b
	Residual	9.702	7	1.386		
	Total	65.630	8			
a. Dependent Variable: ε						
b. Predictors: (Constant), SEI						

Table 4.22 ANOVA results for SCBW-4

ANOVA (SCBW-4)						
Model		Sum of Squares	df	Mean Square	F	Sig.
1	Regression	360.988	1	360.988	165.730	.000 ^b
	Residual	15.247	7	2.178		
	Total	376.235	8			
a. Dependent Variable: ε						
b. Predictors: (Constant), SEI						

Table 4.23 ANOVA results for TBW-1

ANOVA (TBW-1)						
Model		Sum of Squares	Df	Mean Square	F	Sig.
1	Regression	1401.993	1	1401.993	190.276	.000 ^b
	Residual	51.577	7	7.368		
	Total	1453.570	8			
a. Dependent Variable: ε						
b. Predictors: (Constant), SEI						

Table 4.246: ANOVA results for TBW-2

ANOVA (TBW-2)						
Model		Sum of Squares	df	Mean Square	F	Sig.
1	Regression	1060.123	1	1060.123	60.010	.000 ^b
	Residual	123.661	7	17.666		
	Total	1183.783	8			
a. Dependent Variable: ε						
b. Predictors: (Constant), SEI						

Table 25 ANOVA results for TBW-3

ANOVA (TBW-3)						
Model		Sum of Squares	Df	Mean Square	F	Sig.
1	Regression	131.743	1	131.743	143.861	.000 ^b
	Residual	6.410	7	.916		
	Total	138.153	8			
a. Dependent Variable: ε						
b. Predictors: (Constant), SEI						

Table 26 ANOVA results for TBW-4

ANOVA (TBW-4)						
Model		Sum of Squares	df	Mean Square	F	Sig.
1	Regression	887.080	1	887.080	55.044	.000 ^b
	Residual	112.812	7	16.116		
	Total	999.892	8			
a. Dependent Variable: ε						
b. Predictors: (Constant), SEI						

The p-value of SCBW and TBW for all the Tables 4.21 to 4.28, according to the ANOVA tables, is 0.000, or less than 0.001. This shows that there is a substantial correlation between the dependent variable (ϵ) and the independent variable (SEI).

4.4.1.3 Coefficient table

The coefficient table is vital. As it sheds light on the link between the independent and dependent variables, to be more precise, the value of the Beta variable (β) in the Coefficient table indicates the relationship how a one-unit change in the independent variable corresponds to a change in the dependent variable.

Table 27 Coefficient table for SCBW-2

Coefficients (SCBW-2)						
Model		Unstandardized Coefficients		Standardized Coefficients	t	Sig.
		B	Std. Error	Beta		
1	(Constant)	102.791	2.069		49.674	.000
	SEI	-411.835	42.982	-.944	-9.581	.000
a. Dependent Variable: ϵ						

Table 28 Coefficient table for SCBW-3

Coefficients (SCBW-3)						
Model		Unstandardized Coefficients		Standardized Coefficients	t	Sig.
		B	Std. Error	Beta		
1	(Constant)	102.063	1.586		64.364	.000
	SEI	-209.229	32.937	-.913	-6.352	.000
a. Dependent Variable: ϵ						

Table 29 Coefficient table for SCBW-4

Coefficients (SCBW-4)						
Model		Unstandardized Coefficients		Standardized Coefficients	t	Sig.
		B	Std. Error	Beta		
1	(Constant)	104.218	1.988		52.426	.000
	SEI	-531.560	41.291	-.960	-12.874	.000
a. Dependent Variable: ε						

Table 30 Coefficient table for TBW-1

Coefficients (TBW-1)						
Model		Unstandardized Coefficients		Standardized Coefficients	t	Sig.
		B	Std. Error	Beta		
1	(Constant)	87.915	3.656		24.046	.000
	SEI	-1047.560	75.943	-.912	-13.794	.000
a. Dependent Variable: ε						

Table 31 Coefficient table for TBW-2

Coefficients (TBW-2)						
Model		Unstandardized Coefficients		Standardized Coefficients	t	Sig.
		B	Std. Error	Beta		
1	(Constant)	106.409	5.661		18.796	.000
	SEI	-910.928	117.591	-.926	-7.747	.000
a. Dependent Variable: ε						

Table 32 Coefficient table for TBW-3

Coefficients (TBW-3)						
Model		Unstandardized Coefficients		Standardized Coefficients	t	Sig.
		B	Std. Error	Beta		
1	(Constant)	99.547	1.289		77.231	.000
	SEI	-321.122	26.773	-.967	-11.994	.000
a. Dependent Variable: ϵ						

Table 33 Coefficient table for TBW-4

Coefficients (TBW-4)						
Model		Unstandardized Coefficients		Standardized Coefficients	t	Sig.
		B	Std. Error	Beta		
1	(Constant)	95.127	5.407		17.593	.000
	SEI	-833.274	112.314	-.944	-7.419	.000
a. Dependent Variable: ϵ						

The range of β values for both types of breakwaters is found to be between -9.1 and -9.8, according to a review of the coefficient tables (Tables 4.29 – 4.36). This range indicates that there is a comparable change in the dependent variable, ϵ , which ranges from -.91 to -.98, for each unit change in the independent variable, the Shoreline Elevation Index (SEI).

The negative sign associated with these β values shows a negative correlation between SEI and ϵ , as the percentage dissipation tendency (ϵ) of the breakwaters reduces as the Shoreline Elevation Index rises. Understanding the link between ϵ and SEI is essential for comprehending breakwater effectiveness in moderating wave energies throughout coastal locations.

From the statistical analysis using R square, ANOVA table as well as Coefficient table it is proved that the newly introduced non dimensional parameter Shoreline Elevation Index has a significant effect on the wave attenuation tendencies of Breakwaters.

Chapter 5: CONCLUSION AND RECOMMENDATIONS

5.1 Conclusions

In this subject study problem of safeguarding our shorelines and harbors from the damaging effects of marine floods and tsunamis is addressed. Thousands of lives are impacted by these natural calamities every year, this research sought to identify efficient methods for dissipating waves. These investigations were divided into three primary sections. In the beginning, different kinds of breakwaters were contrasted; the solid, non-perforated Semicircular Breakwater (SCBW) and the Triangular Breakwater (TBW). These Breakwaters were tested in a different wave frequencies and water depths, and it was consistently discovered that SCBW performed way better in all scenarios. Moreover, during this experimentation, it was found that frequency of waves and depth of water play a crucial role in boosting Incoming Height of waves therefore position of breakwater matters a lot.

In the second phase, SCBW and TBW were looked again and investigated how they performed at varying perforation percentages. Finding the ideal porosity for maximal wave dissipation was the crux of this category of experimentation. For both kinds of breakwaters, it was found that porosities of 36.6% on the seaside and 22.5% on the shoreside were most ideal. In the same experimental phase, it was found out that freeboard is directly proportional to K_d and inversely proportional to K_r and K_t .

In the last stage, how the breakwaters' placement in relation to the shoreline affected their ability to dissipate waves was investigated. It was discovered that the breakwaters functioned best when they were positioned farthest from the shore after placing each type of breakwater at nine different locations along the shore. A new non dimensional parameter Shoreline Elevation Index (SEI) and examined its effects on the percentage dissipation tendencies of both the breakwaters and found

out that SEI is inversely proportional to the wave dissipation tendency. Furthermore, we employed IBM SPSS Statistics 26 to examine the considerable impact of this new non-dimensional variable, the Shoreline Elevation Index (SEI), on wave dissipation and found out that SEI has direct significant impact on dissipation tendencies of both the breakwaters.

Taking everything into account, this research provides useful knowledge on realistic coastal protection strategies. Our coastal communities may better be safeguarded from the catastrophic consequences of maritime disasters by optimizing the layout and positioning of breakwaters and accounting for factors like porosity and elevation of the coastline.

5.2 Recommendations

Due to growing threat posed by climate change and rising sea levels, there is global concern about mitigating the effects of floods and tsunamis. Our research has demonstrated that addressing these problems necessitates using cutting-edge techniques to calm the waves. In this current experimentation it is found that Semicircular Breakwaters (SCBW) have a clear benefit over triangular breakwater due to its unique shape and angle.

In the subject research, velocities and other related variables were measured with high resolution cameras and automated timers. Particle imaging velocimetry (PIV) is an advanced technique that could have been used in these tests for more accurate and in-depth results, but due to time constraints were not able to use this more advanced technology. Therefore, this method can be applied to the further experimentation to delve deeper into the research to measure the velocity of even tiny water particle's and conduct a thorough analysis of the fluid's behavior and movement once it encounters the breakwaters. Furthermore, a novel non-dimensional parameter called shoreline elevation index (SEI) was proposed in this study. It demonstrated a significant influence

on the % dissipation; hence, a proper relationship could be established to forecast the percentage dissipation using this parameter.

References

- [1] NASA. Warming seas may increase frequency of extreme storms. Nasa Science Editorial Team; 2019.
- [2] Ariyaratne SA. Efficiency of perforated breakwater. 2007.-
- [3] Tanimoto K, Goda Y. Historical development of breakwater structures in the world. Coastal Structures and Breakwaters. 1992.
- [4] Le Xuan T, Le Manh H, Ba HT, Do Van D, Vu HTD, Wright D, et al. Wave energy dissipation through a hollow triangle breakwater on the coastal Mekong Delta. Ocean Engineering. 2022;245:110419.
- [5] JEO. Rising sea level could sink Karachi, displace 40 million people. 2016.
- [6] von Storch H, Woth K. Storm surges: perspectives and options. Sustain Sci. 2008;3:33-43.
- [7] Schiermeier Q. Climate change: A sea change. Nature. 2006;439(7074).
- [8] Haurwitz B. Atmospheric tides. Science. 1964;144:1415-22.
- [9] Davenport J, Davenport JL. The impact of tourism and personal leisure transport on coastal environments: A review. Estuar Coast Shelf Sci. 2006;67(1-2):280-92.
- [10] Saenger P. Mangrove ecology, silviculture and conservation. Springer; 2013.
- [11] Das S, Vincent JR. Mangroves protected villages and reduced death toll during Indian super cyclone. Social Sciences. 2009.
- [12] Sun B, Li C. Experimental and numerical study on the wave attenuation performance. Ocean Engineering. 2022.
- [13] Young AR. Wave transformation over coral reefs. J Geophys Res. 1989.
- [14] Burke L, Spalding M. Shoreline protection by the world's coral reefs: Mapping the benefits to people, assets, and infrastructure. Marine Policy. 2022;146:105311.

- [15] Beck WM. Managing coasts with natural solutions: Guidelines for measuring and valuing the coastal protection services of mangroves and coral reefs. World Bank Group; 2016.
- [16] Dai J, Wang CM, Utsunomiya T, Duan W. Review of recent research and developments on floating breakwaters. *Ocean Engineering*. 2018;158:132-51.
- [17] Flemming N. Cities under the Mediterranean. *Archaeology under Water*. New York: McGraw-Hill; 1980.
- [18] Jensen OJ. A monograph on rubble mound breakwaters. Danish Hydraulic Institute (DHI); 1984.
- [19] Troch P, Rouck JD. Full scale measurements of wave attenuation inside a rubble mound breakwater. *Coastal Engineering*. 1996.
- [20] Mohammadi A, Zakikhani K. Rubble-mound breakwater construction simulation. CSCE Annual Conference. Greater Montreal; 2019.
- [21] Van der Meer JW. Conceptual design of rubble mound breakwaters. *Advances in Coastal and Ocean Engineering*. 1995;1:221-315.
- [22] Jarlan GE. A perforated vertical wall breakwater. *Dock Harb Auth*. 1961;(486):394-8.
- [23] Terrett FL, Osorio JD, Lean GH. Model studies of a perforated breakwater. *Coastal Engineering* 1968. 1968;1104-20.
- [24] Massel S, Mei C. Transmission of random wind waves through perforated or porous breakwaters. *Coastal Engineering*. 1977.
- [25] Kondo H. Analysis of breakwaters having two porous walls. *Coastal Structures' 79*. ASCE; 1979.
- [26] Kakuno S, Oda K, Liu PLF. Scattering of water waves by vertical cylinders with a backwall. *Coastal Engineering* 1992. 1993;1258-71.
- [27] Isaacson M, Baldwin J, Allyn N, Cowdell S. Design of a perforated breakwater. *Ports' 98*. ASCE; 1998;1189-98.
- [28] Isaacson M, Baldwin J, Allyn N, Cowdell S. Wave interactions with perforated breakwater. *J Waterw Port Coastal Ocean Eng*. 2000;126(5):229-35.
- [29] Zhu S, Chwang AT. Investigations on the reflection behaviour of a slotted seawall. *Coastal Engineering*. 2001.

- [30] Li Y, Dong G. The reflection of oblique incident waves by breakwaters with. Coastal Engineering. 2003.
- [31] Liu Y, Li Y. Wave interaction with a new type perforated breakwater. Acta Mech Sin. 2007.
- [32] Ariyaratne HA. Efficiency of perforated breakwater and associated energy dissipation [dissertation]. Texas A&M University; 2008.
- [33] Garrido JM, Medina JR. Study of reflection of perforated vertical breakwaters. Resgate. 2007.
- [34] Rageh OS, Koraim AS. Hydraulic performance of vertical walls with horizontal slots used as breakwater. Coastal Engineering. 2010;57(8):745-56.
- [35] Huang Z, Li Y, Liu Y. Hydraulic performance and wave loadings of perforated/slotted coastal structures: A review. Ocean Engineering. 2011;38(10):1031-53.
- [36] Shih RS. Experimental study on the performance characteristics of porous breakwaters. Ocean Engineering. 2012.
- [37] Marks W. A perforated mobile breakwater for fixed and floating application. Coastal Engineering. 1966.
- [38] Elbisy MS. Wave interactions with multiple semi-immersed Jarlan-type perforated breakwaters. China Ocean Eng. 2017;31:341-49.
- [39] Haleem DA, Muhammed JR. Inclined porous screen walls performance. Fifth Int Eng Conf Dev Civil Comput Eng Appl. 2019.
- [40] Tamrin, Pallu S. Experimental study of perforated concrete block. Int J Eng Technol IJET-IJENS. 2014;14(3).
- [41] Tanimoto K, Takahashi S. Design and construction of caisson breakwaters—the Japanese experience. Coastal Engineering. 1994.
- [42] Xie SL. Design of semi-circular breakwaters and estuary jetties. Proc Int Assoc Hydraul Res. 2001;90-95.
- [43] Yuan D, Tao J. Wave forces on submerged, alternately submerged, and emerged semicircular breakwaters. Coastal Engineering. 2003;48(2):75-93.
- [44] Christou M, Swan C, Gudmestad OT. The interaction of surface water waves with submerged breakwaters. Coastal Engineering. 2008;55(12):945-58.

- [45] Testik FY, Young DM. Onshore scour characteristics around submerged vertical and semicircular breakwaters. *Coastal Engineering*. 2009.
- [46] Young DM, Testik FY. Wave reflection by submerged vertical and semicircular breakwaters. *Ocean Engineering*. 2011.
- [47] Teh HM, Venugopal V, Bruce T. Hydrodynamic performance of a free surface semicircular perforated breakwater. *Coastal Eng Proc*. 2010;32:20-20.
- [48] Venugopal T, Min H. Performance analysis of composite semicircular breakwaters. *Coastal Engineering*. 2012.
- [49] Liu Y, Li HJ. Analysis of oblique wave interaction with a submerged perforated semicircular breakwater. *J Eng Math*. 2013;83:23-36.
- [50] Liu Y, Li HJ, Zhu L. Bragg reflection of water waves by multiple submerged semi-circular breakwaters. *Appl Ocean Res*. 2016;56:67-78.
- [51] Jiang XL, Zou QP, Zhang N. Wave load on submerged quarter-circular and semicircular breakwaters under irregular waves. *Coastal Engineering*. 2017;121:265-77.
- [52] Dong L, Watanabe A, Isobe M. Nonlinear wave transformation over a submerged triangular breakwater. *Coastal Engineering* 1996. 1996;2324-37.
- [53] Weisberg M. *Simulation and similarity: Using models to understand the world*. OUP USA; 2013.
- [54] Katell G, Eric B. Accuracy of solitary wave generation by a piston wave maker. *HAL Open Sci*. 2002.
- [55] Renouard D, Santos FS. Experimental study of the generation, damping, and reflection of a solitary wave. *Dyn Atmos Oceans*. 1985;341-58.
- [56] Zelt J, Skjelbreia JE. Estimating incident and reflected wave fields using an arbitrary number of wave gauges. *Coastal Engineering*. 2015.
- [57] Van der JW, Daemen IF. Stability and wave transmission at low-crested rubble-mound structures. *Ocean Eng*. 1994.
- [58] Meer JW, Briganti R. Wave transmission and reflection at low-crested structures: Design formulae, oblique wave attack and spectral change. *Coastal Eng*. 2005.
- [59] Burcharth HF, Hughes SA. Types and functions of coastal structures. *Coastal Eng Man*. 2003;VI-2.

- 、
- [60] Dean RG. Water wave mechanics for engineers and scientists. Adv Ser Ocean Eng. 1984;2:353.
- [61] Seed HB, Rahman MS. Wave-induced pore pressure in relation to ocean floor stability of cohesionless soils. Mar Georesour Geotechnol. 1978;3(2):123-50.